La Sapienza

Università di Roma

Facoltà di Scienze Matematiche, Fisiche, Naturali

DOTTORATO DI RICERCA IN BIOLOGIA CELLULARE E DELLO SVILUPPO

XXX CICLO

Increasing Antigen Presenting Cells at the injection site improves SAM Vaccine Efficacy

PhD student: Cristina Manara

Docente guida: Prof.ssa Loretta Tuosto

Tutor: Dr. Elisabetta Frigimelica

Coordinatore**:** Prof.ssa Giulia De Lorenzo

ANNO ACCADEMICO 2017/2018

Table of Contents

ABBREVIATIONS

Ab	Antibody
Ag-	Antigen
APC	AlloPhyco-Cianin
APCs	Antigen Presenting Cells
BHK	Baby Hamster Kidney
BMDM	Bone marrow derived monocytes
BSA	Bovine Serum Albumin
CFSE	CarboxyFluorescein Succinimidyl Ester
CMTMR	5-(and-6)-(((4ChloroMethyl)benzoyl)amino) TetramethylRhodamine
CMV	Cytomegalovirus
CNE	Cationic Nanoemusion
CTLs	Cytotoxic T Lymphocytes
DCs	Dendritic Cells
DLS	Dynamic Light Scattering
DMEM	Dulbecco's modified Eagle's Medium
dsRNA	Double strand RNA
EDTA	Ethylenediaminetetraacetic acid
ELISA	Enzyme-Linked Immunosorbent Assay
EU/ml	ELISA units per ml
FACS	Fluorescence-Activated Cell Sorting
FBS	Fetal Bovine Serum
FITC	Fluorescein IsoThioCyanate
GFP	Green Fluorescent Protein
GM-CSF	Granulocyte Macrophage Colony Stimulating factor
GOI	Gene of interest

HEPES	Hydroxyethyl piperazineethanesulfonic acid
His	Histydine
HRP	Horseradish peroxidase
ICS	IntraCellular Staining
IFNs	Interferons
IgG	Immunoglobulin G
I.m.	Intramuscular
LiCl	Lithium Chloride
LNP	Lipid NanoParticle
mAb	Monoclonal Antibody
MDCK	Madin-Darby Canine Kidney
MOPS	N-morpholino) propanesulfonic acid
mRNA	Messenger RNA
mutGM-CSF	Mutant GM-CSF
MW	Molecular Weight
Ni-NTA	Nickel-Nitrilotriacetic acid
NP	Nucleoprotein
OVA	Ovalbumin
PBS	Phosphate Buffered Saline
pDNA	Plasmid DNA
PNGase F	Peptide N-Glycosidase F
PR8	Influenza virus A/PR/8/1934
PVDF	PolyVinyl DiFluoride
RPMI	Roswell Park Memorial Institute
RT	Room Temperature
SAM	Self-Amplifying RNA
scFv	Single chain fragment variable

SDS- PAGE	Sodium Dodecyl Sulfate Polyacrylamide gel electrophoresis
TCID50	Tissue Culture Infectious Dose
VRP	Viral Replicon Particle

ABSTRACT

Self-amplifying mRNAs (SAM) based vaccines are effective at eliciting potent and protective immune responses. The SAM technology is developed as a platform technology with the potential to be used for a broad range of targets, able to induce both cellular and humoral response. Recently published data demonstrate that bone marrow derived Antigen Presenting Cells (APCs) are responsible for CD8 T cell priming after SAM vaccination, even though these cells are not able to express antigen directly from the SAM construct. This suggests cross-priming is a key mechanism for antigen presentation by SAM vaccines. Professional APCs are a key target for strategies aimed to enhance the immunogenicity of vaccines because of their specific ability to capture, process and present Ags to T cells. One successful approach for targeting these APCs is to increase the number of antigen loaded APCs at the injection site.

Since GM-CSF is a chemoattractant for APCs, we developed a SAM(GM-CSF) vector and administered it intramuscularly in mice together with another SAM construct encoding the influenza A virus nucleoprotein [SAM(NP)]. We hypothesized that the presence of GM-CSF together with the NP antigen would lead to increased APCs recruitment and to an increased NP-specific CD8 T cell response. We indeed observed that administration of the SAM(GM-CSF) vector enhances the recruitment of APCs (DCs and macrophages or monocytes) in the draining lymph nodes and at injection site. Moreover, co-administration of SAM(GM-CSF) with SAM(NP) significantly improves the magnitude of NP-induced CD8 T-cell responses both in frequency of cytotoxic $CD8^+$ T cells and in functional activity in an *in vivo* cytotoxicity assay.

A second strategy addressed in the present study, in order to enhance the potency of SAM vaccines, is to target the antigen of interest directly to surface receptors expressed on cross-presenting DCs. Fusion constructs are made of single chain fragment variable (scFv) or ligands that bind surface receptors expressed on DCs fused to OVA antigen. These fusion constructs have been designed, expressed and tested *in vitro* for their binding activity to DCs.

INTRODUCTION

Nucleic Acid Vaccines

A key advancement in vaccinology has been the use of Vectors based on recombinant viruses (viral vectors). Safe and efficacious virus, such as vaccinia or adenovirus, are genetically modified in order to include genes encoding for immunogenic proteins from other pathogens and induce specific immunological responses against these antigens *in vivo* [1]. Viral vectors show several advantages over traditional vaccine technologies: they offer an efficient delivery of nucleic acid to the host cell using pathways of entry employed by the pathogen. In this way vectors mimic a live viral infection, with reduced safety risks associated with live organisms. Some of them are also able to deliver antigens directly to components of the immune system such as antigen presenting cells [2]. Moreover, they have intrinsic adjuvant effects due to the expression of pathogen associated molecular patterns which activate innate immunity. The main drawback of viral vectors is that the effectiveness of the vaccine may be reduced by pre-existing or vaccination-induced immunity to the viral envelope [3].

As an evolution of viral vectors, nucleic acid-based vaccines have emerged as alternative platform. They involve direct immunization with DNA or RNA encoding the antigen, which is synthetized *in situ*, and inducing an immune response directed only toward the antigen of interest. Both DNA and RNA-based vaccines do not generate immunity to the envelope, can be used for multiple doses, and are easy to produce, reducing manufacturing cost [2].

DNA (deoxyribonucleic acid) vaccination uses antigen-encoding DNA plasmid to produce an immunological response. This DNA plasmid can induce an immune response against parasites, bacteria and viruses [4, 5, 6]. The expression of the antigen-encoding gene can be increased by adding various promoters, enhancers and other elements to the backbone of plasmid DNA [4, 5, 7]. More than two decades of research studies have already demonstrated the effectiveness of

plasmid DNA vaccines to elicit antibody and T cell-mediated protection in animal models. However, DNA-based vaccines still have some limitations due to the weak immunogenicity in humans compared to small animal models [8, 9] and for the potential risk of DNA integration into the host genome.

For these reasons, RNA-based vaccines have emerged as a safer and more potent alternative to DNA vaccines.

RNA-based vaccines

RNA-based vaccines have emerged as a promising alternative to plasmid DNA for gene vaccination [2, 10, 11]. RNA vaccines show some clear advantages over plasmid DNA. Unlike DNA, RNA is delivered directly into the host cytoplasm where it is translated avoiding the limiting step of crossing the nuclear membrane and the potential risk of genome integration. Moreover, RNA is produced *in vitro* using a cell-free enzymatic transcription reaction, avoiding safety concerns associated with the use of living organisms or anti-vector immunity associated with the use of viral vectors [12, 13].

RNA Vaccines show also an intrinsic adjuvant activity by activating members of the Toll Like receptors family that can induce innate immune responses, involving type I interferons (IFNs) [14, 15, 16].

Currently, there are two major forms of RNA vaccines: conventional non-amplifying mRNA molecules and self-amplifying mRNA, characterized by a replicative activity, derived from RNA viruses.

Non-amplifying RNAs consist of a cap structure, an open reading frame encoding the gene of interest flanked by a 5’ and 3’ untranslated regions (5’ UTR and 3’ UTR), and a tail of adenosine residues (poly(A) tail) (Figure 1). They offer the advantages of the small size (2-3 kb), the simplicity of the construct and the absence of additional proteins, which excludes the possibility of undesired responses. However, non-amplifying mRNAs are poorly immunogenic *in vivo* [17],

probably because of their short half-life and instability that result in low level of antigen expression. Self-amplifying mRNAs were developed with the aim to extend the duration and magnitude of expression of the antigen of interest.

Self-amplifying mRNAs, also called replicons, are derived from either positive- or negative-stranded RNA virus like alphaviruses (Sindibis, Semliki Forest, and Venezuelan equine encephalitis viruses) or flaviviruses (Yellow fever, Kunjin) [18, 19, 20, 21, 22]. Self-amplifying mRNAs contain the basic elements of conventional mRNAs as described above, a large ORF encoding four nonstructural proteins (nsP1-4) that allow the amplification of the RNA, and a subgenomic promoter upstream of the gene of interest (GOI) that replaces the genes encoding the viral structural proteins, avoiding the production of infectious viral particles (Figure 1). RNA replicons are effective at eliciting humoral and cell-mediated immune responses in different animal models including mice [17], non-human primates [23], and humans [24], and they have been tested against several target diseases. The main disadvantage of RNA-based vaccines is their instability. Therefore, one of the most important challenges for RNA-based vaccines is to find effective delivery systems in order to prevent RNA enzymatic degradation and to facilitate the transfection of host cells. RNA replicons can be packaged into virus-like particles by supplying the structural proteins *in trans* in cell culture. These viral replicon particles (VRPs) are unable to produce new infectious particles and are effective at inducing potent immune responses in different animal models and humans, however, their clinical application is limited by safety concerns related to cell culture production. Therefore, several means of non-viral delivery have been explored, including inorganic particles, polymeric-based vectors and cationic lipid-based vectors, or physical methods such as electroporation and gene gun delivery [25].

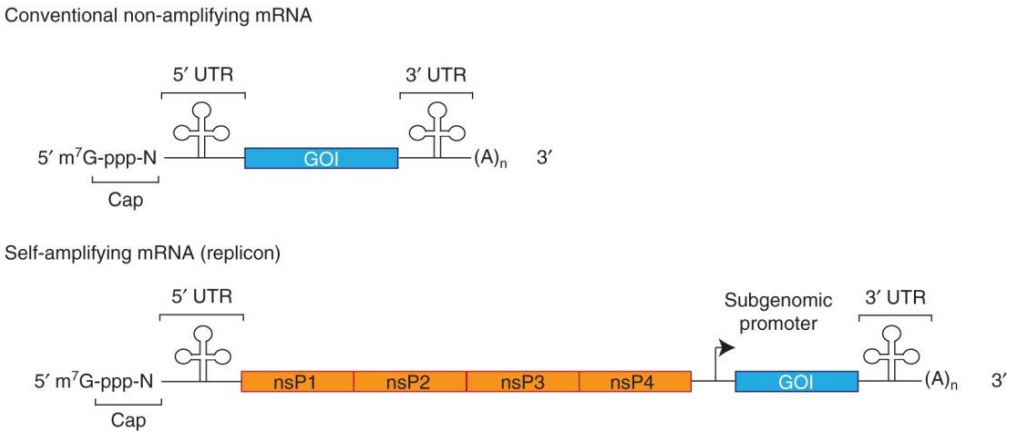

Deering RP et al, *Expert Opin Drug Deliv* 2014

Figure 1
Structural elements of RNA-based vaccines

Schematic illustration of a conventional non-amplifying mRNA (upper figure) containing the cap structure, the 5' UTR region, an open reading frame encoding the gene of interest (GOI), 3' UTR and a poly(A) tail, and of a self-amplifying mRNA (lower figure) derived from an alphavirus genome, containing the basic elements described above, an ORF encoding four non-structural proteins (nsP1-4), and a subgenomic promoter upstream to the GOI. [26]

SAM Vaccines

The SAM Vaccine platform, first developed by Novartis Vaccines and later acquired by GSK Vaccines, is based on the non-viral delivery of a synthetic, self-amplifying mRNA. This 9-kb self-amplifying mRNA is derived from an engineered alphavirus genome containing the genes encoding the alphavirus RNA replication machinery [27] whereas the structural protein sequences are replaced with genes encoding protein antigens, which are abundantly expressed from a subgenomic promoter in the cytoplasm of cells transfected with these self-amplifying RNAs (Figure 2) [28, 29, 30].

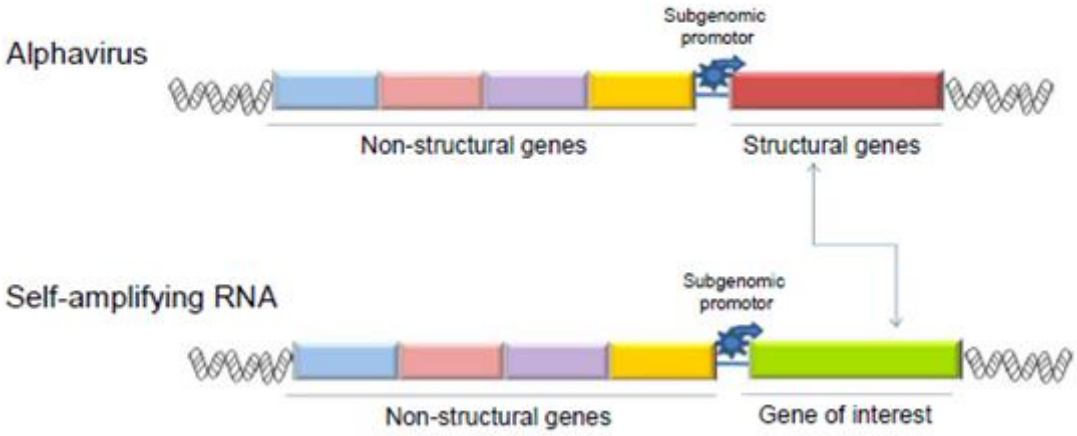

Rofriguez-Gascon A. et al, Int J Nanomedicine 2014

Figure 2
Self-amplifying RNA derived from an alphavirus

Scheme showing a self-amplifying RNA derived from an alphavirus in which structural genes have been replaced by the gene of interest

The RNA is produced *in vitro* by an enzymatic transcription reaction from a linearized pDNA template using a T7 RNA polymerase.

To provide protection from degradation, and to facilitate entry into cells, a non-viral delivery of self amplifying mRNA was explored. Geall and colleagues took advantage of a clinically suitable delivery system for short interfering RNA (siRNA) based on the use of synthetic lipid nanoparticle LNP [31, 32]. Cationic lipids and mRNA are mixed together to obtain stable particles that prevent RNA enzymatic degradation and deliver the mRNA into host cells by interacting with the negatively charged cell membrane (Figure 3).

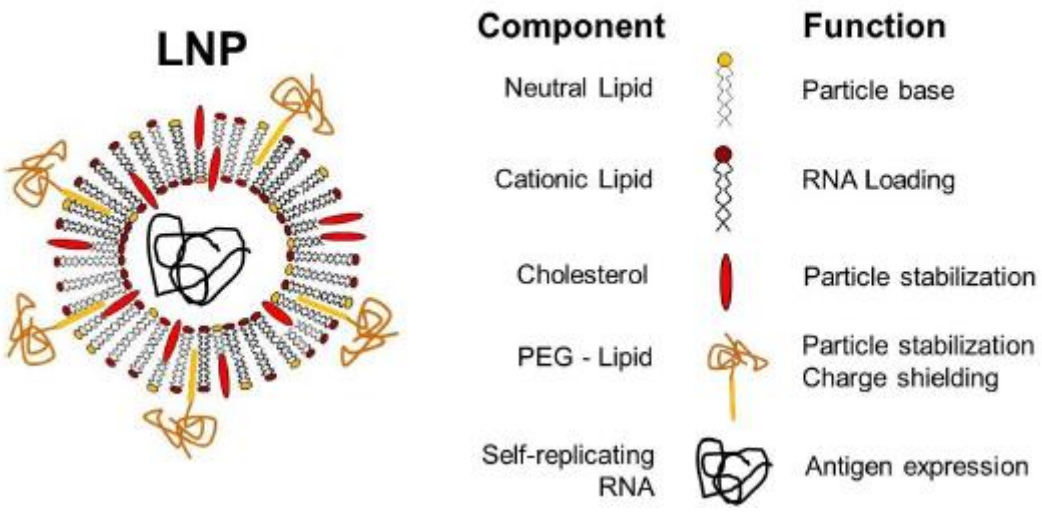

Geall A.J. et al., *PNAS* 2012

Figure 3
SAM Vaccines LNP formulates

Schematic illustration of a lipid nanoparticle (LNP) encapsulating self-amplifying RNA Lipid components and relative functions are indicated.

Once in the cytoplasm, the RNA polymerase, encoded by the non-structural genes of the viral replicon, is expressed and produces a negative-sense copy of the genome that is used as template for the amplification of the genome, as well as for the transcription of the sub-genomic mRNA encoding the vaccine antigen (Figure 4). Encapsulation of the self-amplifying RNA in LNPs was shown to protect it from enzymatic degradation, assure efficient RNA delivery after intramuscular injection and increase the immunogenicity compared to injection of naked (unformulated) RNA [33].

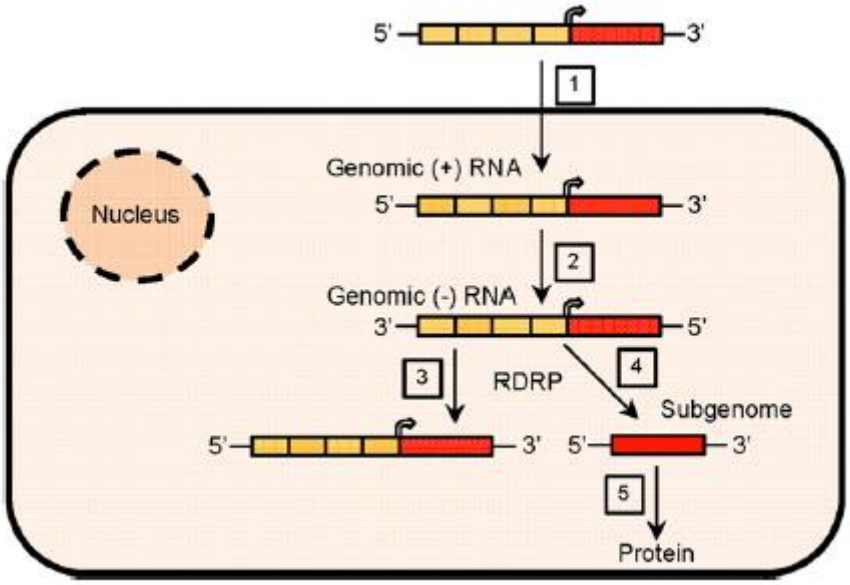

Figure 4

Schematic illustration of the steps in replication and expression of self-amplifying RNA after delivery to a mammalian cell.

(1) Delivery of RNA to thecytoplasm. (2) Translation of the ORF encoding the four nonstructural proteins that form the RNA-dependent RNA polymerase (RDRP), which produces a negative-sense copy of the genome. (3) RDRP catalyses production of positive-sense genomes from the negative sense copy. (4) RDRP catalyses transcription of subgenome. (5) Translation of the gene of interest, leading to protein expression.

An alternative non-viral delivery system is based on a cationic nanoemulsion (CNE), which binds to the SAM RNA, enhances its delivery, and thereby substantially increases the potency of the vaccine. CNE is composed of the cationic lipid DOTAP (1,2-dioleoyl-sn-glycero-3-phosphocholine), chosen for its previous clinical use and fixed positive charge, emulsified with the constituents of the emulsion adjuvant MF59, which is currently licensed in 30 countries and is well tolerated in children and adults. CNE was demonstrated to be an effective system able to induce immune responses in multiple animal species, including rhesus macaques, at comparable levels to responses elicited by an adjuvanted subunit vaccine or VRP delivery of the same RNA, and at doses much lower than those required for pDNA vaccines [25].

The discovery that lipid-based formulations could be used to deliver self-amplifying mRNA vaccines brought a completely new approach to vaccine production using a simple, synthetic, rapid and cell-free process. These attributes make the SAM technology an attractive rapid response platform for the health challenges of the 21st century.

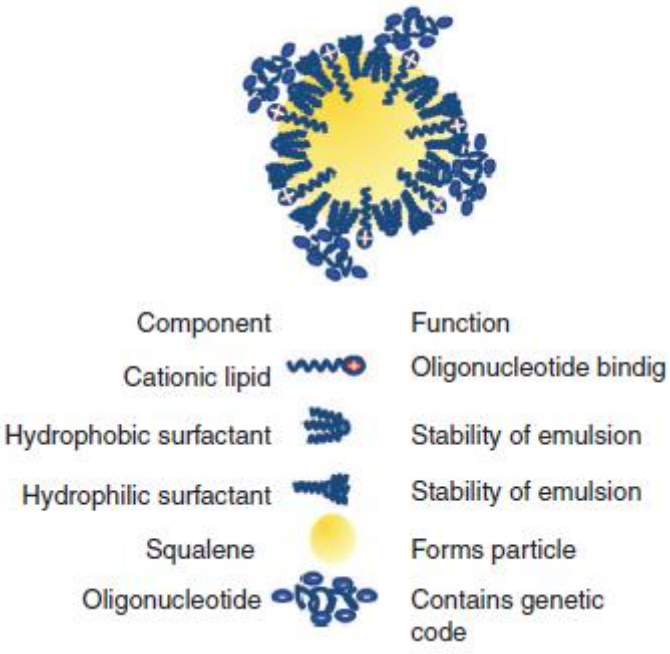

Brito LA et al, *Mol Ther* 2014

Figure 5

SAM Vaccines CNE formulated

Schematic illustration and role of components of CNE in complex with SAM RNA.

Mechanism of action

SAM vaccines demonstrated to induce functional immune responses against different infectious targets in multiple animal models, including non-human primates (NHPs). Preclinical proof of concept has so far been achieved for Influenza, Respiratory syncytial virus, Rabies, Ebola, Cytomegalovirus, Human

immunodeficiency virus and Malaria [33, 34, 25, 35]. However, little has been published on the mechanism of action of these vaccines. Recently published studies show that myocytes appear to be the predominant cell type transfected after SAM immunization but are not able to prime CD8 T cells; while it seems that bone marrow-derived professional APCs do not express directly the antigen but are required for the *in vivo* priming of MHC class-I restricted CD8 T cells. Therefore, a possible mechanism suggests that APCs could acquire the antigen from transfected myoblasts, implicating cross-priming as a mechanism for priming CD8 T cell response by SAM vaccines. However, the cellular mechanism by which cross-priming occurs *in vivo* still needs to be clarified. One hypothesis is that transfected cells at the site of injection undergo apoptosis during RNA amplification, leading to the release of the antigen associated apoptotic bodies, which are then phagocytosed by APCs and presented via MHC class-I restricted pathway. The published data strongly suggests cross-presentation by APCs of myocyte-derived antigens is the primary mechanism for priming CD8 T cells. However it cannot be excluded that some APCs are directly transfected by SAM vaccines but express the antigen under the limit of detection of the assays used in the studies [36].

Cross-priming and cross-presentation

$CD8^+$ cytotoxic T lymphocytes (CTLs) play a pivotal role in the immune defence against intracellular pathogens or tumours. These cells recognize tumor- or pathogen-derived antigenic peptides associated with MHC class I molecules, which are expressed on the surface of all cells in the body. When effector CTLs detect the specific peptide being presented by an infected or cancer cell, they destroy the cell to avert the spread of infection or cancer. The endogenous MHC class I pathway is reserved for peptides derived from intracellularly synthesized proteins. Naive antigen-specific CD8+ T cells need to be activated by professional antigen-presenting cells (APCs), usually dendritic cells (DCs), before they can

exert their cytotoxic effector functions. So when an intracellular pathogen does not directly infect APCs or when a tumour is not APC-derived (which is the case for most tumours), naive antigen-specific CD8+ T cells can only be activated by an APCs presenting the exogenous antigen on MHC class I molecules. This process, termed cross-presentation, was named after the phenomenon of cross-priming discovered in the 1970s by Bevan [37], in which antigens from intravenously injected cells 'crossed' into the MHC class I pathway of host APCs for CTL priming. Cross-priming has been shown to be required for defence against many viruses and tumours [38, 39], and it is essential for vaccinations with protein antigens, which must be cross-presented to activate CTLs [40] (Figure 6). Under normal circumstances, cross-presentation is probably less efficient than direct presentation, since cross-presentation requires the additional step of transfer from one cell to another. Apoptotic cells have been reported to be a good antigen source for cross-presentation *in vitro* [41, 42, 43], and recent studies also show a role for necrotic cells [41, 44] (Fig.6).

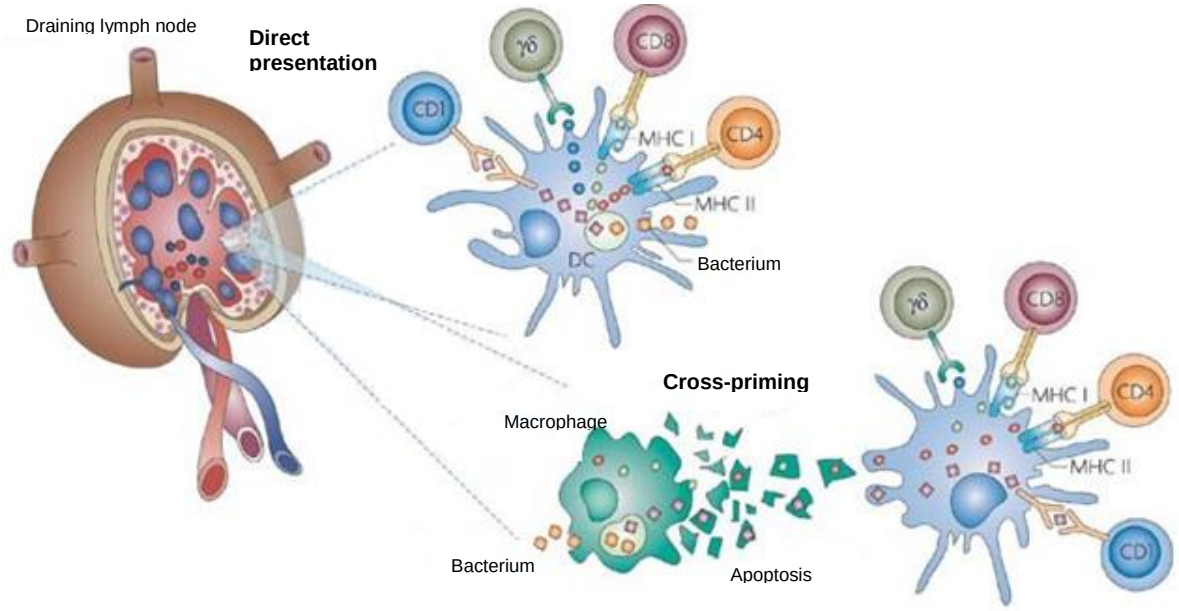

Kaufmann SHE, *Nat Rev Microbiology* 2007

Figure 6

Antigen presentation to different T-cell subsets: direct presentation and cross-priming.

Direct antigen presentation leads to unrestricted stimulation of $CD4^+$ T cells, γδT cells and CD1-restricted T cells. However, some bacteria have developed evasion mechanisms that impair direct antigen presentation. As most bacterial pathogens reside in the phagosome, direct major histocompatability complex (MHC) class I presentation of antigen for $CD8^+$ T cells is impaired. Only bacterial pathogens that egress into the cytosol allow for direct antigen presentation to $CD8^+$ T cells. Cross-priming was originally described as a pathway that allows MHC class I presentation of exogenous antigens to $CD8^+$ T cells. It was later extended to include antigen presentation from bacterial pathogens.

Roles of APC types in cross-priming.

Despite the discovery of cross-priming in the 1970s, the phenotype of the APC responsible for this process remained unknown for long time.

Bevan and colleagues [45] provided the first evidence that $CD8a^+$ DCs are responsible for cross-priming *in vivo* in mice. Although $CD8^+$ DCs now seem to be the predominant cross-presenting subset, it has been shown that under inflammatory conditions also DCs that lack the expression of CD8a can cross-present, suggesting that this mechanism is influenced by the surrounding environment. Recent studies have proposed, as a possible mechanism, that cross-presentation takes advantage of distinct endocytosis pathways able to introduce the antigen directly into the organelle (or organelles) in which cross-presentation occurs [46]. In support of this, it has been shown that the uptake of antigens for cross-presentation is restricted to distinct endocytosis receptors, such as Fc receptors and certain members of the C-type lectin receptor family, such as C-type lectin 9A (CLEC9A; also known as DnGR1), CLEC7A (also known as dectin 1), DC-SIGN (also known as CD209), DEC205 (also known as CD205) , mannose receptor 1 (also known as CD206) and XC-chemokine receptor 1 (XCR1) [47, 48,

49, 50, 51]. These receptors are expressed by CD8α+ DCs [46], providing a possible mechanistic explanation for why this DC subset can cross-present.

GM-CSF

Following intramuscular injection of SAM vaccine, most antigen expression occurs in transfected myocytes at the inoculation site. However, recent evidence suggests that T cell priming is initiated by professional APCs rather than myocytes [36]. Since professional APC are not typically found in normal muscle tissue, they presumably migrate to the site of inoculation in response to inflammatory or chemotactic signals. Then, infiltrating APCs present the SAM expressed antigen by both direct and cross presentation to initiate immune responses. Since APCs are present in low number at the injection site, to enhance antigen uptake by DCs, and therefore presentation, one of the strategies that has proven to be successful in the literature is to increase the number of antigen-loaded APCs at the injection site. For this purpose, GM-CSF has received considerable attention given its ability to enhance cellular immune responses specific for a variety of antigens. Granulocyte-macrophage colony-stimulating factor (GM-CSF) is a pleiotropic cytokine responsible for the proliferation, differentiation, and activation of macrophages, neutrophils, and various APCs [52, 53, 54]. GM-CSF is produced by various cell types, including T cells, B cells, macrophages, mast cells, endothelial cells, fibroblasts, and adipocytes, in response to cytokine or inflammatory stimuli. GM-CSF can stimulate and enhance the production and function of neutrophils and monocytes. The adjuvant activity of GM-CSF is partly mediated by chemo-attraction and activation of APCs, which triggers antigen internalization, processing and presentation to lymphocytes [55]. Furthermore, by increasing the number and maturation state of DCs and by promoting their ability to cross-present antigens, GM-CSF can enhance the immune responses to vaccines (Figure 7). GM-CSF was first identified as an adjuvant for antitumor vaccines. Dranoff and colleagues reported that irradiated tumor cells transfected

with the gene encoding murine GM-CSF increased protection in mice upon immunization [56]. Subsequently, GM-CSF has been used as a vaccine adjuvant in a number of immunization systems; as a recombinant protein, GM-CSF has been injected locally or systemically [57, 58, 59, 60, 61] or in conjunction with hydrogel [62, 63]; dendritic cells (DCs) have been cultured in the presence of recombinant GM-CSF [64, 65] or transfected with the GM-CSF gene [66] and used to immunize mice [64, 66] or humans [65]; and plasmid-encoded GM-CSF (pGM-CSF) has been used for DNA vaccination studies with the GM-CSF gene either linked to an Ag-encoding gene [67] as a bicistronic plasmid [68] or as a separate plasmid mixed with the Ag encoding plasmid [69, 70, 71, 72, 73, 74].

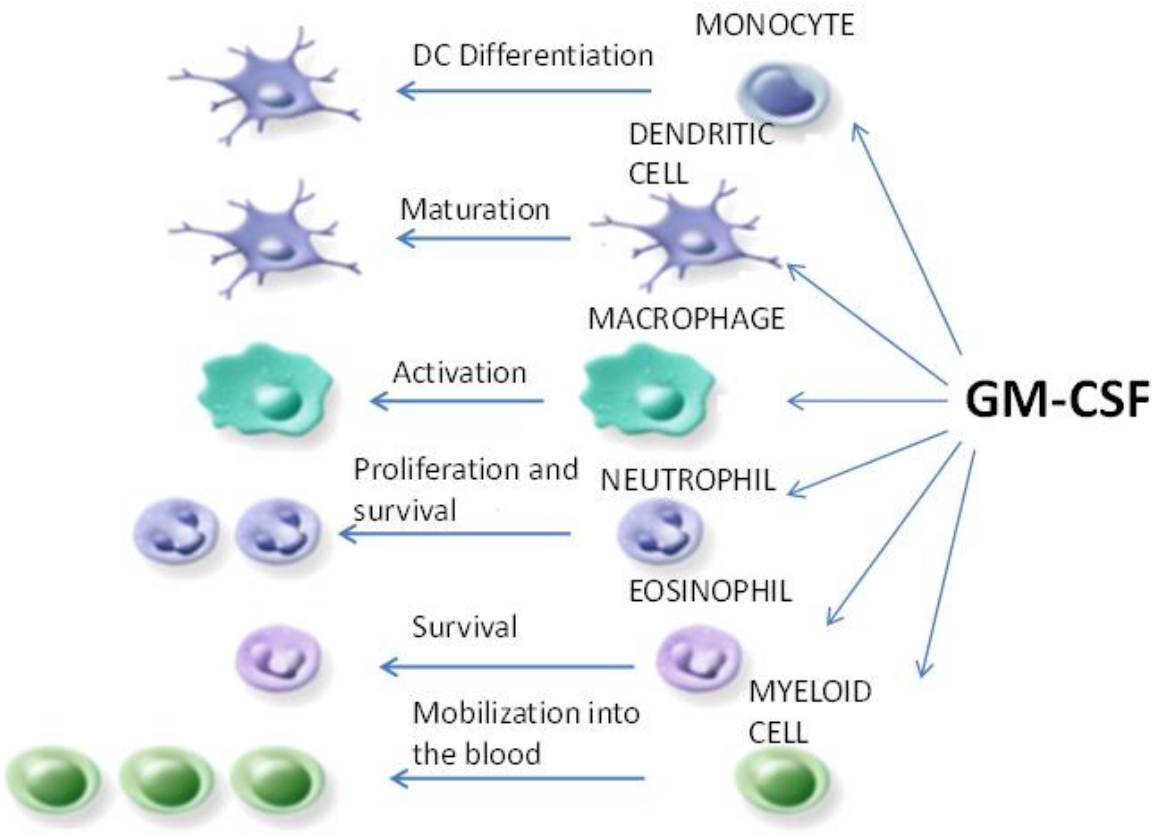

Kaufman et al, *J. Immunotherapy of Cancer* 2014

Figure 7

Immunobiologic effects of GM-CSF

Effects of GM-CSF on cells of the immune system

Targeting Antigens to Dendritic Cells receptors

The superior ability of cross-presenting DCs to stimulate adaptive immunity suggests that an enhanced immune response could be gained from targeting antigens directly to this DCs population *in vivo* [75, 76]. The most widely studied approach involves the selective targeting of DCs by linking the antigen of interest to antibodies (in the form of either monoclonal antibodies or single chain variable fragment, scFv) or ligands that specifically bind to their endocytic receptors. Following internalization by the targeted DCs, the intracellular routing of these complexes depends on the specific receptor targeted, and has functional consequences regarding the antigen presentation and T cell stimulation (Figure 8).

Targeting antigens to DCs-specific receptors may reduce the required vaccine dose and reduce the portion of the vaccine dose that ends up in non-target cells, thus diminishing potential adverse effects. To date, more than 100 DC-targeting studies have been published [77]. The first DC-targeting studies in mice were aimed at Fcγ receptors (FcγRs), MHC class II molecules and CD40 [78, 79, 80], and showed that antigen targeting improves both humoral and cellular adaptive immunity. During the last decade, research has focused on C-type lectins and, in particular, CD205 (also known as LY75) has been extensively studied in mice, NHPs and humans.

DEC-205 is a C-type lectin that delivers ligands to late endosomal/lysosomal compartments and it has been proven to be especially effective at inducing CD8+ T cell responses [81]. This suggests that antigen-targeting to DEC-205 might be useful for inducing protective CTL-based immunity in diseases such as cancer, malaria, and HIV.

As CD8α+ DCs are superior at cross-presentation, targeting this DC subset is advantageous for inducing CD8+ T cell responses. The human orthologue of this DC subset lacks CD8α, but expresses CLEC9A, XCR1 and blood DC antigen 3 (BDCA3; also known as CD141 and thrombomodulin) [82, 83, 84, 85, 86]. In particular, the ability of CLEC9A and XCR1 to target CD8α+ DCs in mice makes these receptors the most promising candidates for the induction of CTL responses.

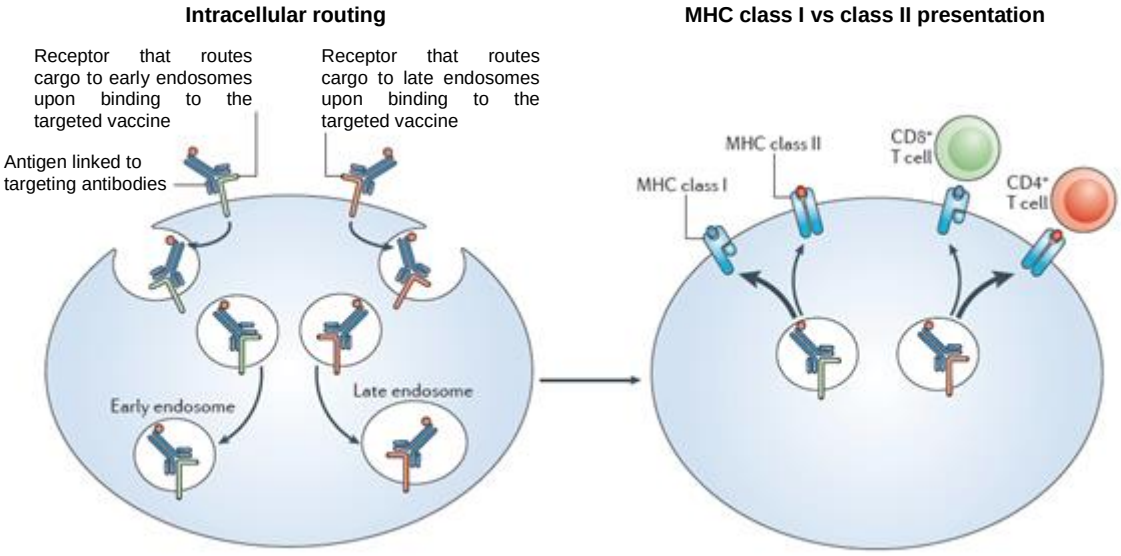

Kastenmüller W et al., *Nat Rev Immunology* 2014

Figure 8

Antigen presentation and intracellular routing.

Targeting antigens via surface receptors leads to internalization of the receptor together with its cargo. The intracellular routing depends on the receptor and has important functional consequences for antigen presentation. Most receptors are routed to late endolysosomes in which antigen is quickly degraded and efficiently presented on MHC class II molecules to $CD4^+$ T cells. Some receptors route their cargo to early endosomes in which antigen is slowly digested, leading to prolonged MHC class I presentation to $CD8^+$ T cells [87] [88] [89]. Thicker arrows indicate that the pathway of antigen presentation is more efficient.

RATIONAL AND AIM

SAM vaccines are emerging as a promising technology platform able to generate potent, versatile and easily produced vaccines to address the health challenges of the 21st century [66, 67, 70, 71, 79].

The mechanism by which SAM vaccines activate the host immune system has not been deeply investigated. Recently published data suggests that bone marrow derived Antigen Presenting Cells (APCs) are responsible for CD8 T cell priming after SAM vaccination. Since muscle fibers express antigens after SAM immunization, but APCs are not directly transfected by the SAM construct, cross-priming is proposed as the key mechanism for antigen presentation by SAM vaccines.

The aim of the current study was to explore strategies to further potentiate the SAM platform. Assuming the pivotal role of APCs for the induction of the immune response, and taking into account the low amount of APCs present at the injection site, we wanted to investigate 2 different strategies to enhance the immune response induced by SAM vaccine: on one side by increasing the recruitment of APCs at the site of injection and on the other side to target the antigen specifically to DCs.

In the literature, the enhancement in the number of APCs has been obtained in different ways and using different chemoattractants; in particular, GM-CSF has been selected among different possible molecules as an important hematopoietic growth factor and immune modulator

Our first aim was to investigate whether an increase in the number of Antigen presenting cells at the injection site could improve the immunogenicity to a model antigen by using GM-CSF expressed by SAM vector as chemoattractant.

The model antigen chosen for the study was Ovalbumin protein and later on the Nucleoprotein from Influenza A Virus was used to obtain more complete data on the immunogenicity and to investigate also the effect of SAM(GM-CSF) on the protective efficacy after an Influenza challenge.

A secondary aim of the present study was to evaluate whether targeting specifically the antigen of interest to DCs, we could obtain an increase in the immune response. The targeting is obtained by using fusion constructs made of scFV or ligand that bind surface receptors expressed on DCs , and fused to OVA antigen.

MATERIALS AND METHODS

Cloning and RNA synthesis of vaccine antigens

Mouse GM-CSF coding sequence (Gene ID: 12981) was codon optimized for expression in mouse by GeneArt. The synthetic gene was amplified using forward primer 5'-acatagtctagtcgacgccaccatgtg-3' and reverse primer 5'gggcgtagcggcggccgctgggtgggcgcgccg-3'. The coding sequence of GM-CSF was mutated at amino acids 15 (H to A) and 21 (E to A) by PCR SOEing using the following primers: forward primer 5'-gccgtggaagccatcaaagccgccctgaacctgctggacgac-3' and reverse primer 5'-ggctttgatggcttccacggccttccagggtctggtcacgg-3'. This mutant form of GM-CSF (mutGM-CSF) has lost the ability to bind to the GM-CSF receptor and lacks bioactivity [74, 90] .

The SAM (NP) construct was described previously [36, 91].

The coding sequence of Ovalbumin (Gene ID: 100303699) was truncated from aa 1 to 144, to obtain a cytosolic expression, as described elsewhere [92]. The sequence was PCR amplified by using forward primer 5'-tctagtcgacgccaccatgttccagacagctgccga-3' and reverse primer 5'-cgtagcggcggccgctggtcagggtgacacgcagcg-3'.

All the amplicons were then cloned as a *Sal I* and *Not I* fragment into the SAM vector.

Plasmid DNA encoding NP, Ovalbumin, GM-CSF and mutGM-CSF were amplified in Escherichia coli and purified using the Qiagen Plasmid Maxi kit Endo free (Qiagen). DNA was linearized immediately downstream the 3' end of the replicon by endonuclease digestion with *Pme I* for NP and OVA, with *BspQ I* for GM-CSF and mutGM-CSF, and purified by phenol/chloroform extraction and ethanol precipitation. Linearized DNA templates were transcribed into RNA using the MEGAscript T7 transcription kit (LifeTechnologies), following manufacturer's instructions, and purified by LiCl precipitation. RNA was then capped using the ScriptCap m7G Capping System (CellScript) and purified again by LiCl

precipitation. RNA was resuspended in RNAse free water and its integrity was evaluated on 1% denaturing agarose-LE gel (Ambion).

For protein purification, GM-CSF and mutGM-CSF sequences were cloned into a pCMV vector with a 6-His tag at the C terminus. SAM vector encoded sequences were PCR amplified with forward primer 5'-agtctagtcgacgccaccatgtg-3' and reverse primer 5'- atatctagattagtgatggtgatggtgatgcttctggccgggtttcttgc-3' and then cloned as *Sal I* and *Xba I* fragments into a pCMV expression vector.

RNA vector self-amplification and protein expression assessment

Baby hamster kidney cells (BHK, ATCC) were cultured in Dulbecco's modified Eagle's
medium (Gibco, Carlsbad, CA) containing 5% fetal bovine serum (Euroclone) at 37°C and 5% CO2, and used at 80% confluence at the time of transfection.
To determine the efficiency of RNA self-amplification, $1x10^6$ trypsinized BHK cells were electroporated (120V, 25ms pulse) with 200 ng of RNA and incubated for 16–18 h at 37°C and 5% CO2. Cells were then stained with Live/Dead Aqua (Invitrogen), fixed and permeabilized with Cytofix/Cytoperm (BD Biosciences), and stained with APC-conjugated anti-double stranded (ds) RNA antibody (J2 monoclonal mAb mouse IgG2a kappa chain, Bioclass). Anti-dsRNA IgG2a was conjugated using the Zenon Allophycocianin labeling kit (Invitrogen). For NP protein expression, an anti-NP antibody conjugated to FITC (Thermo Fisher) was used. Frequencies of dsRNA+ cells and NP+ cells were measured by flow cytometry on a FACS CANTO II flow cytometer (BD Biosciences).

For Western blot analyses, 16-18h post-transfection supernatants were collected and BHK cells were trypsinized and lysed in 1X Loading sample buffer (Novagen). Supernatants and whole cell lysates of $2x10^5$ cells were subjected to SDS-PAGE under reducing conditions and blotted to nitrocellulose membranes. GM-CSF and mutGM-CSF were detected with a polyclonal rabbit anti-mouse GM-CSF antibody (1:2500 dilution; Abcam), Ovalbumin with a polyclonal rabbit anti-Ovalbumin

(Abcam), followed by horseradish peroxidase-conjugated goat anti-rabbit IgG secondary antibody (1:5000 dilution; Dako). Protein bands were visualized by chemiluminescence following manufacturer's instructions (GE Health Care, Life sciences).

The supernatants of BHK cells transfected with SAM (GM-CSF) were subjected to PNGase treatment 1h at 37° in order to check the glycosylation pattern of the expressed GM-CSF.

Expression and Bioactivity of GM-CSF

Expi 293T cells were transfected with pCMV encoding GM-CSF His-tagged protein and mutGM-CSF His-tagged, according to manufacturer's instructions. Supernatants were collected 48 h after transfection and tested for protein expression by Western Blot analysis. A combination of polyclonal rabbit-anti-GM-CSF (Abcam) and goat-anti-rabbit-HRP (Dako) antibodies was used for detection. Both proteins were purified from supernatants of transfected cells by Ni-NTA-affinity chromatography as described by the manufacturer (Qiagen).

The ability of the purified GM-CSF to generate DCs from bone marrow cultures was tested. Bone marrow derived monocytes (BM-DCs) were induced from BM cells obtained from 5-6 weeks-old C57Bl/6 mice as previously described [93]. Briefly, a single cell suspension was prepared from BM obtained from femurs. $2x10^6$ BM cells were cultured in RPMI 1640 medium (Gibco) supplemented with 25 mM HEPES (Gibco), 10% heat inactivated FBS (low endotoxin, HyClone), 1x Pen/Strep/Glut (100x, Gibco), 50 µM β-mercaptoethanol (Sigma) and 10 ng/ml His tagged mouse GM-CSF (a mouse recombinant GM-CSF from Miltenyi was used as a positive control at the same concentration) in 10 cm diameter Petri dishes at 37 °C in 5% CO2. Supplemented medium was replaced every three days. On day 8, non-adherent cells were collected and analyzed by FACS. The differentiated cells were characterized by surface staining with the antibodies anti-CD80 PECF594, anti-CD86 FITC (all BD Bioscience), anti-CD11c APCeFluor780, anti-F4/80 eFluor450 and anti-Gr1 PercPCy5.5 (all eBioscience) in FACS analysis.

Mice

Animals were housed in the GSK Vaccines Animal Facility and experiments were conducted in compliance with the ARRIVE guidelines, the current Italian legislation (Legislative Decree 116/92), and with the GSK Animal Welfare Policy and Standards.

Female C57Bl/6 mice (Charles River Laboratories, Calco, Italy), aged 5–6 weeks, were immunized intramuscularly (i.m.) on day 0 in the quadriceps muscles of both hind legs (25 µl vaccine formulation per leg) with 1.5 µg of each formulated RNA, in combinations described in details for each experiment.

CNE/RNA formulation

CNE was prepared as previously described [25]. Each RNA was formulated independently as follows: RNA was diluted in the appropriate buffer at a concentration of 300 µg/ml and was then added to an equal volume of CNE. The complex was mixed gently and allowed to complex on ice for 30 min. Prior to administration, formulations were diluted to dosing concentrations and mixed when indicated. Formulations were characterized for particle size and RNA integrity (using gel electrophoresis) as previously described [25]. Dynamic light scattering was used to determine CNE particle size. CNE was diluted 1:500 in PBS and added to disposable low volume cuvettes (Malvern). Samples were measured on a Malvern NanoZs Zetasizer with a backward angle measurement using “PBS” as a dispersant (RI = 1.330). For RNA integrity, the RNA were extracted from the CNE56 by addition of 25 µl formulated sample to 475 µl isopropanol (Sigma). After 30 minutes of centrifugation at maximum speed, the pellet was suspended in nuclease free water (Ambion) and 1X Glyoxal Loading Dye (Ambion). The RNA were analyzed by gel electrophoresis on mini gel (MOPS/Sodium Acetate/EDTA buffer) 1% agarose and run at 100V.

Immune cell infiltrate in quadriceps muscles and draining lymph nodes

C57Bl/6 mice aged 5–6 weeks (eight mice per group) were inoculated in the quadriceps muscles of the two hind legs (25 µl per site) on day 0. On day 1, 2, 3, 4, 7, 10, 25 mice were sacrificed and both of the quadriceps muscles and draining inguinal lymph nodes were collected. Quadriceps muscles and lymph nodes were then dissociated into single cell suspensions and analyzed by flow cytometry for immune cell infiltrate composition. To obtain single cell suspension, quadriceps muscles were digested with the enzyme mix provided by the Skeletal Muscle Dissociation kit (Miltenyi) for 1h at 37 °C under constant agitation. The resulting cell suspensions were centrifuged, resuspended in Dulbecco's modified Eagle's medium (Gibco) and filtered through 70 µm nylon mesh (BD) before staining.

Lymph nodes were dissociated by using a mix of Liberase DL research Grade (Roche) and DNAse I (Sigma) for 90 minutes at 37 °. The resulting cell suspensions were filtered through a 30 µm filter and then washed with PBS before staining. The single cell suspensions, from muscles and lymph nodes were stained with Live Dead Yellow (Invitrogen) and the following fluorescently labeled antibodies: anti-Ly6C FITC, anti-CD11b PE-Cy7, anti-Ly6G PE, anti-CD8 α APC, (all from BD Pharmingen) and anti-MHCII AlexaFluor700, anti-F4/80 eFluor450, anti-CD11c APC-AlexaFluor780, (all from eBioscience) and anti-CD3PerCPCy5.5(BD Biosciences). The stained cells were acquired on a LSR II Special Order System flow cytometer (BD Biosciences) using BD DIVA software (BD Bioscience). The different cell subsets were identified following the gating strategy shown in Figure 9 and 10.

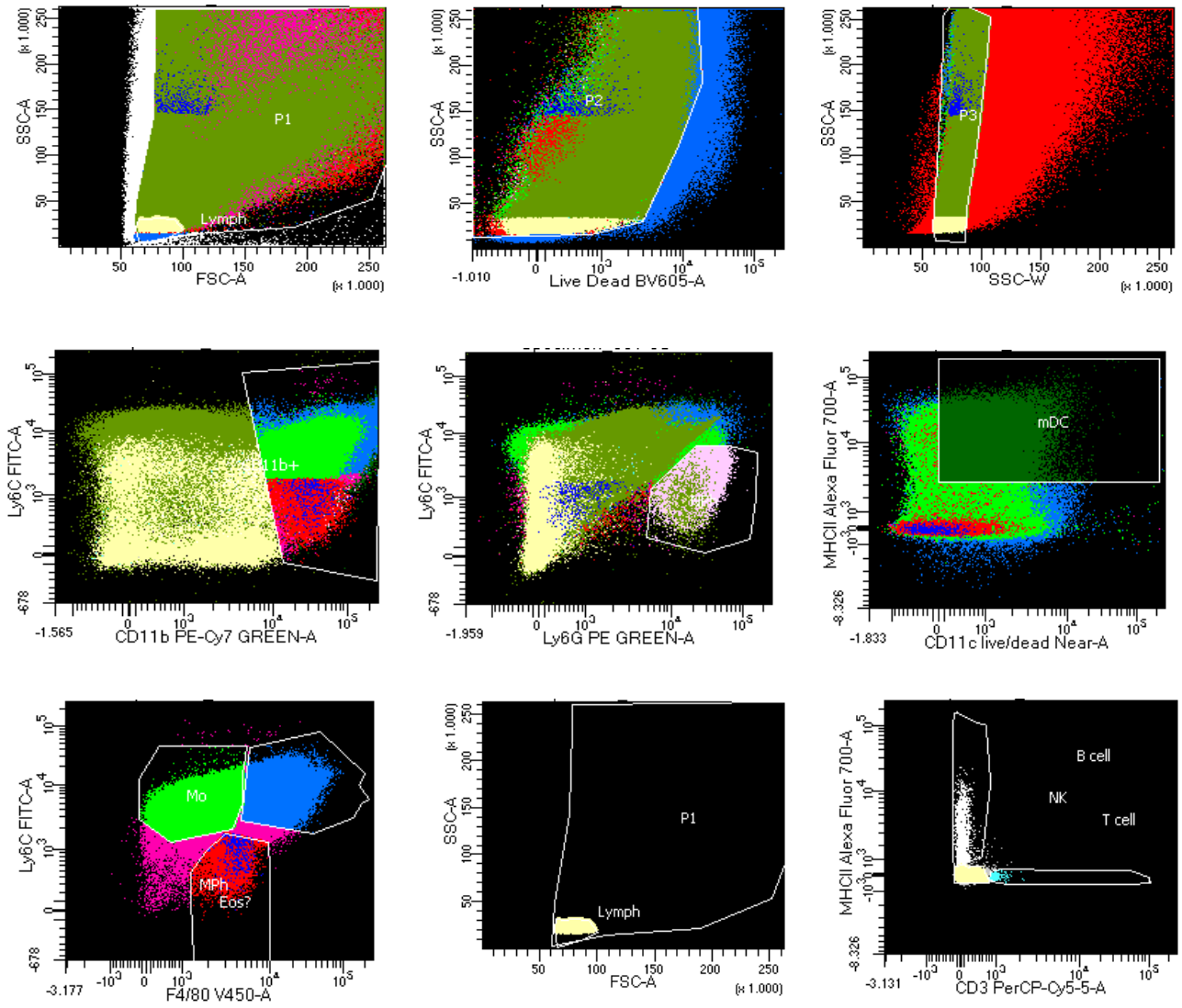

Figure 9

Gating strategy for the identification of cells recruited in the muscles after SAM administration.

Live cells were negatively selected based on Live/Dead dye exclusion, and immune cells were further identified based on morphology. After discrimination of singlets, $CD11b^+$ cells were selected. Among them, neutrophils are identified as double positive for Ly6C and Ly6G expression. After exclusion of NPh, Dendritic cells (DCs) cells were selected as $MHCII^+/CD11c^+$.

After exclusion of DCs, monocytes , macrophages and eosinophils were identified.

Lymphocytes were selected based on morphology and among them T ($CD3^+/MHCII^-$), B ($CD3^-/MHCII^+$) and NK ($CD3^-/MHCII^-$) cells were discriminated.

Representative dot plots are shown.

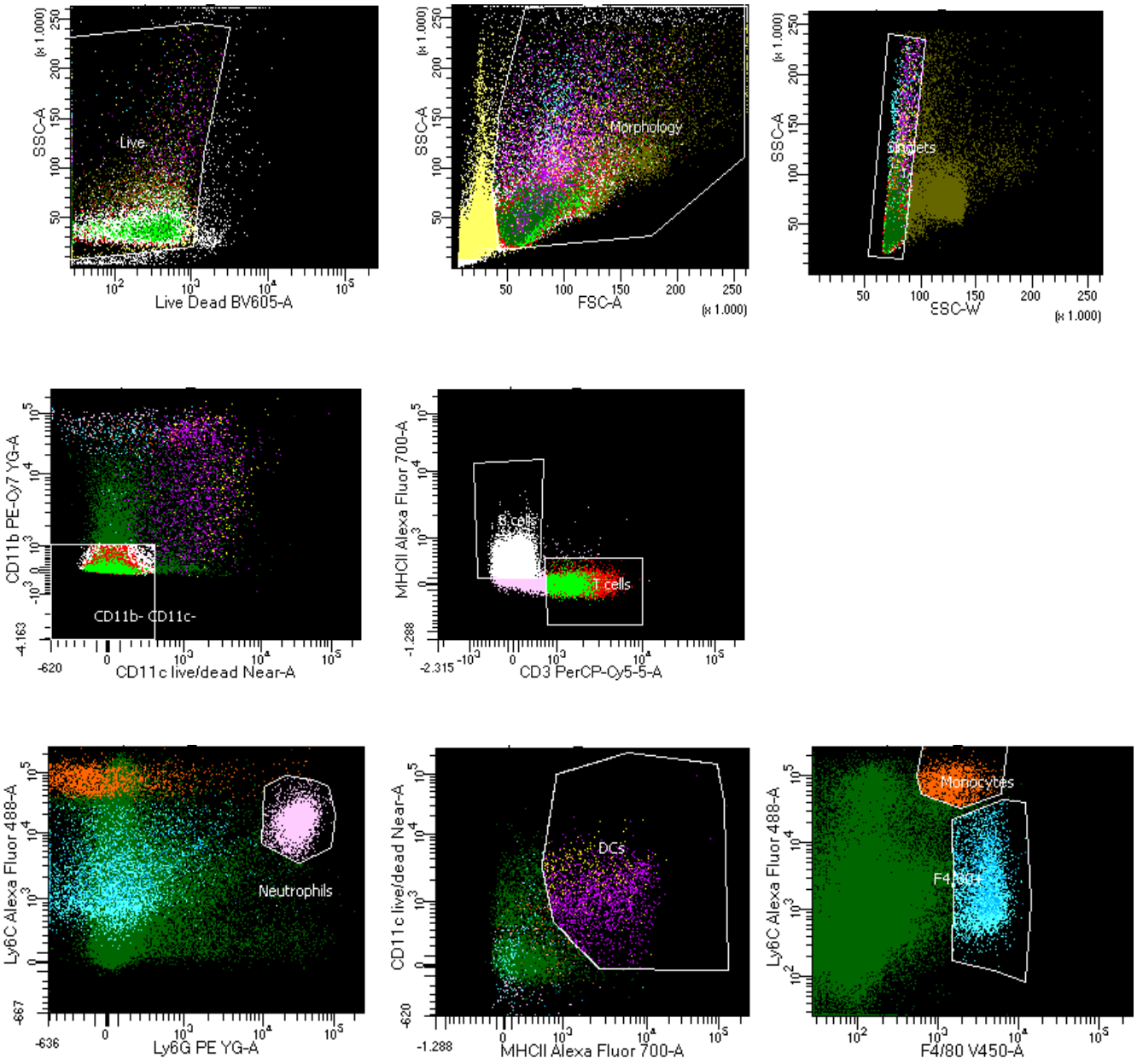

Figure 10
Gating strategy for the identification of cells recruited in the lymph nodes after SAM administration.

Live cells were negatively selected based on Live/Dead dye exclusion, and immune cells were further identified based on morphology. After discrimination of singlets, CD11b-/Cd11c- cells were selected. Among them B cells were identified as CD3-/MHCII +, while T cells as $CD3^{+}$/MHCII -. On $CD11b^{+}$/$CD11c^{+}$, Dendritic cells (DCs) cells were selected as $MHCII^{+}$/$CD11c^{+}$. After exclusion of DCs, neutrophils (Nph) were visualized based on Ly6C

and Ly6G expression. After exclusion of Nph, monocytes were identified as LY6C^{+} F480^{int} and macrophages (Mph) as Ly6C$^{low\ int}$/F4/80^{+}.

Determination of cytokine concentration in sera

At indicated time points after the immunization, sera samples were collected. A panel of 23 cytokines, both pro-inflammatory and anti-inflammatory, were evaluated using the Luminex Bio-Plex Pro Mouse Cytokine 23-Plex Immunoassay (Bio-Rad), according to the manufacturer's protocol.

ELISA

NP-specific, OVA-specific or GM-CSF-specific IgG titers were determined on sera collected 3 weeks after the immunization. 96–well Maxisorp plates (Nunc) were coated with 0.26 µg/well of NP Protein (Sinobiological), 0,1 µg/well of OVA protein (Sigma) or 0,1 µg/well of GM-CSF protein(Miltenyi) at 4°C overnight. On the next day, plates were washed with PBS/0.05% Tween 20 and blocked with PBS/1% BSA for 2 h at room temperature. Serum samples and a standard serum were 2-fold serially diluted in PBS, 1% BSA, 0.05% Tween 20, then transferred into coated and blocked plates and incubated 2 h at RT. Plates were washed and incubated with an alkaline phosphatase-conjugated goat anti-mouse IgG (Sigma) for 2 h at room temperature. Then the P-nitrophenyl phosphate substrate was added and the reaction was stopped by using 3% EDTA pH 8. Absorbance was measured with an Infinite M200 plate reader (Tecan) at 405 nm. The IgG titers were normalized with respect to the standard serum assayed in parallel and are indicated as ELISA Units/ml (EU/ml).

Spleen processing

Spleens were harvested from C57Bl/6 mice 10 days after immunization and placed in 5 ml of cold RPMI 1640 medium (Gibco) supplemented with 25 mM HEPES (Gibco), 2% heat inactivated FBS (Euroclone) and 1x Pen/Strep (100x, Gibco) in a 15 ml tube. Spleens were dissociated using the pestle of a 5 ml syringe through a 70 µM cell strainer placed on top of a 50 ml Falcon tube. Red blood cells were lysed by incubating the cell pellet with 1 ml of lysis buffer (eBiosciences) for 3 min at room temperature. The reaction was stopped by adding 9 ml of RPMI. After centrifugation at 300 x g for 5 minutes, splenocytes were suspended in 4 ml of medium: RPMI 1640 (Gibco) supplemented with 25 mM HEPES (Gibco), 10% heat inactivated FBS (low endotoxin, HyClone), 1x Pen/Strep (100x, Gibco) and 50 µM β-mercaptoetanol (Sigma). Cell suspension was filtered on a 30 µm strainer and cell counts determined using an hemocytometer.

Intracellular cytokine staining (ICS)

To assess antigen-specific T-cell responses, single-cell suspensions were prepared from spleens of immunized mice as described above. $2x10^6$ splenocytes were plated in 96w plates together with anti-CD28 mAb (2 µg/ml; Pharmingen), anti CD-49 mAb (2 µg/ml; eBioscience) and with anti-CD107a FITC conjugated (2.5 µg/ml; BD Biosciences). Cells were stimulated for 6 h with H2-D^b-restricted NP peptide ASNENMETMESS (2.5 µg/ml; JPT), or with the recombinant NP protein (5 µg/ml; Sino Biological Inc.), or with H-$2K^b$-restricted (SIINFEKL) or I-A^d-restricted (ISQAVHAAHAEINEAGR) OVA peptides (InvivoGen) all diluted in reaction medium. The same number of cells was incubated with anti-CD3 mAb and anti-CD28 mAb (Pharmingen, 1mg/ml each) as positive control. Brefeldin A (5 µg/ml; Sigma) was added for the last 4 h. For flow cytometry analyses, cells were stained with Live/Dead Near InfraRed (Invitrogen), fixed and permeabilized with

Cytofix/Cytoperm (BD Biosciences), and then incubated with anti-CD16/CD32 Fc block (BD Biosciences). Cells were further stained with anti–CD4 V500 (eBioscience), anti-CD3 APC, anti–IFN-γ^{+} Brilliant Violet 785, anti–IL-2 PE-Cy5.5, anti–TNFα^{+} Brilliant Violet 605 (All from Biolegend), anti–CD44 V450 (BD Horizon), and anti-CD8 PE Texas Red (Invitrogen). Samples were acquired on a LRSII special order (BD Biosciences), and analyzed using FlowJo software version 9.9.5 (LLC). T cells were identified following the gating strategy shown in Figure 11. Frequencies of antigen-specific T cells were calculated after subtracting the background measured in the corresponding negative control (incubated with medium only) for each cytokine.

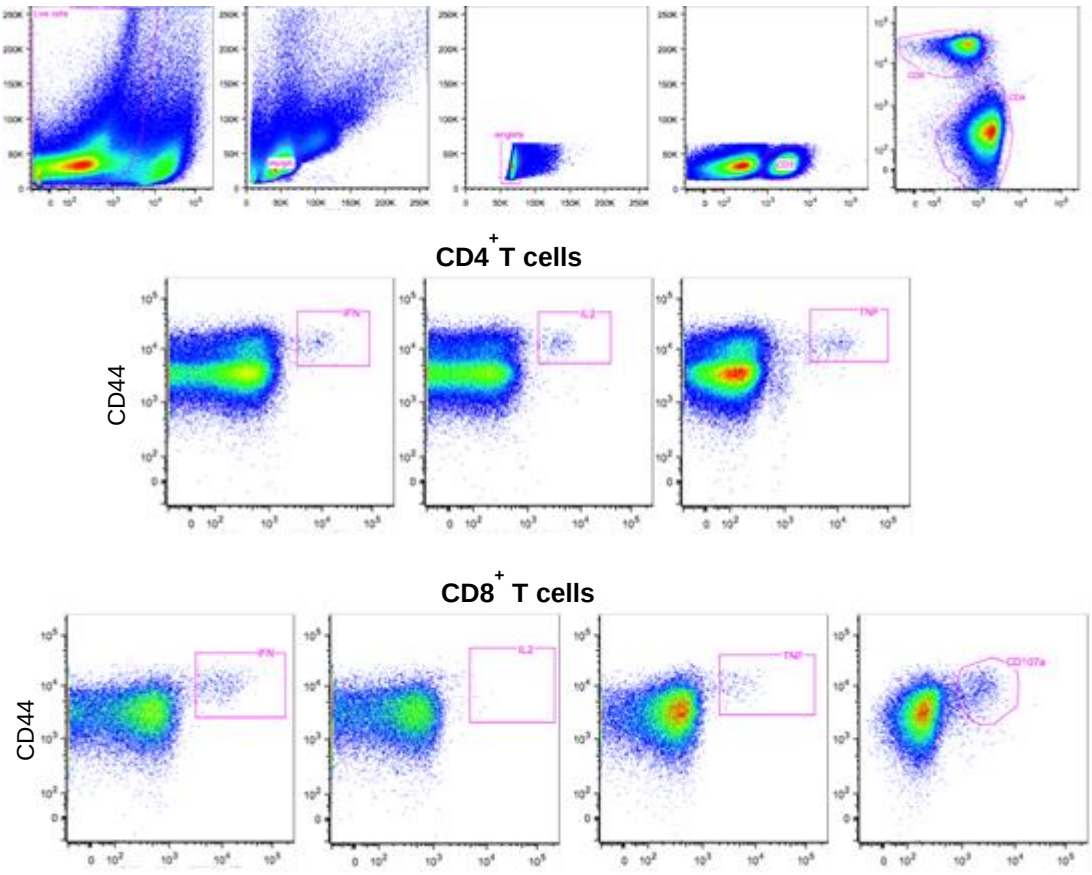

Figure 11
Gating strategy for flow cytometry analyses of CD4 and CD8 T-cell responses

Live cells were negatively selected based on dye exclusion, and lymphocytes were further identified based on morphology. $CD3^+$ T cells were selected after discrimination of singlets and CD4 and CD8 T cells were
identified based on $CD4^+$ and $CD8^+$ expression, respectively. $Cytokine^+$ (IFN-γ, IL-2 and TNFα) and $CD107a^+$ cells were identified among the $CD4^+CD44^{high}$ and $CD8^+CD44^{high}$ T cell subsets.
Representative dot plots are shown.

In vivo cytotoxicity assay

Groups of 6 C57Bl/6 mice were immunized as described above. To prepare target cells, spleens from naïve mice were processed as described above and splenocytes were split into two populations. One population was pulsed for 1 h at 37°C with 5 µM of $NP_{366-377}$ peptide (ASNENMETMESS), washed, and labeled with 0.5 µM of CFSE for 15 min at RT ($CFSE^+$ cells). The other population was pulsed with an unrelated $OVA_{257-264}$ peptide (SIINFEKL), and labeled with 10 µM of CMTMR for 30 min at 37°C (CMTMR+ cells). An equal number of cells (4 $x10^6$ total splenocytes) from the two different peptide-pulsed and labeled populations was mixed and injected intravenously into immunized mice 10 days after the first immunization. After 18 h, mice were sacrificed and collected splenocytes were stained with Live dead Near InfraRed and then analyzed on a LRSII Special order System (BD Biosciences) to determine the frequencies of $CFSE^+$ and $CMTMR^+$ cells.
The percentage of target cell killing was determined as previously reported [94] : 100 − ((percentage of peptide-pulsed targets in immunized mice/percentage of unpulsed targets in immunized mice)/(percentage of peptide-pulsed targets in PBS control mice/unpulsed targets in PBS control mice) × 100).

Influenza virus challenge

Four weeks after the immunization, anesthetized mice were challenged intranasally with a
lethal dose of Influenza A Virus PR8 (H1N1) (38.5 TCID50) mouse-adapted influenza virus (15 µl per nostril). Survival, body weight, and clinical signs of illness (e.g. ruffled fur, hunched posture, hypothermia, body weight loss, wheeze) were monitored daily for 2 weeks after the infection. A clinical score of 4 and a body weight loss superior than 25 % of the initial weight were defined as humane endpoint; animals meeting these criteria were euthanized.

Statistical analysis

Statistical analyses were performed using GraphPad Prism 7.0 software. Experiments involving animal survival were analyzed by Mantle-Cox Log-rank test. For the other statistical analyses, Mann-Whitney U test was used. P values less than 0.05 were considered statistically significant. *, $P<0.05$; **, $P<0.01$; ***, $P<0.001$.

Cloning and purification of fusion constructs

The expression constructs encoding the fusion constructs to target OVA antigen to DCs were obtained as follows. To generate scFv anti DEC-205-OVA and scFv anti Clec9a-OVA, the cDNA of the heavy and light chain variable regions of the monoclonal antibody NLDC-145 (US 2004/0146948) and of the monoclonal antibody 10B4 (US 8,426,565） respectively were assembled with a $(Gly4Ser)_3$ encoding linker and synthesized by GeneArt. The sequences were amplified by PCR from the GeneArt constructs to yield 750 bp long single-chain fragments. The

scFvs were fused to OVA full length coding sequence by PCR SOEing (scFv anti-DEC205-OVA and scFv anti-Clec9a-OVA), separated by a glycine serine linker (GSGGGG). XCL1-OVA was obtained by fusing the full length murine XCL1 coding sequence (Gene ID: 16963) to OVA full length, separated by the glycine-serine linker. To try to improve the binding of the 3 different fusion proteins to DCs, OVA coding sequence was put at the N-terminus of each construct (OVA-scFv anti-DEC205, OVA-scFv antiClec9a and OVA-XCL1). A 6-His tag was added at the C-terminus of each of the fusion construct to facilitate the detection and purification. The resulting products were then cloned into a pCMV expression plasmid containing a murine Ig k chain leader sequence. Supernatants collected from Expi293 T cells transfected with 30 µg of each fusion construct expression plasmids were subjected to affinity chromatography purification by using Ni-NTA columns. Protein production and purification were analyzed by SDS PAGE gel electrophoresis and Western blotting using an anti-OVA antibody.

In vitro binding assay

To evaluate the binding of the fusion proteins to DCs, spleens from naïve C57Bl/6 mice were collected and processed as described above. $3x10^6$ cells were washed with PBS and incubated for 30 minutes at 37° with the different fusion constructs to test (30 µg/ml each). As negative control, the cells were incubated with OVA protein only. Cells were washed with PBS 3 times and incubated on ice for 30 minutes with an anti-OVA-FITC conjugated antibody. The cells were washed again 3 times with PBS and then stained on ice with anti-CD11c-APCe780 conjugated, anti-MHCII A700 conjugated, anti-CD8a PECF594 conjugated antibodies for 30 minutes. After 2 washes with PBS, mouse DCs were identified by FACS as $CD11c^+$ and $MHCII^+$ cells. Gating on these DCs, we identified the CD8+ DCs and among them the cells positive for the anti-OVA antibody.

RESULTS

PART I

Generation and *in vitro* characterization of SAM constructs

To determine whether an increased number of Antigen presenting cells at the injection site could improve the immunogenicity to a model antigen, GM-CSF was selected as chemoattractant. For this purpose, GM-CSF was cloned in the SAM vector: briefly the mouse GM-CSF coding sequence was codon optimized for expression in mouse by GeneArt and amplified by PCR from the synthetic gene. A control plasmid encoding a non-active form of mouse GM-CSF (altered at two amino acids, 15 and 21, required for binding to the GM-CSF receptor) was constructed by PCR SOEing. The NP gene was amplified from the reverse-transcribed RNA genome of influenza virus A/PR/8/34. The coding sequence of Ovalbumin was truncated from aa 1 to 144 and then PCR amplified. All the 4 different genes were cloned using *Sal I Not I* restriction sites into the SAM DNA plasmid backbone containing the promoter for the T7 bacteriophage RNA polymerase (Figure 12, a).

Linear plasmid DNAs were transcribed into RNA through the *in vitro* transcription reaction and a guanine nucleoside (cap) was added to the 5' terminus of primary RNAs with the *in vitro* capping system as reported in Materials and Methods. The quality and the integrity of purified RNAs were assessed by agarose gel electrophoresis: bands of the expected molecular weight (9Kb) and no signs of degradation were observed (Figure 12, b)**.**

The self-amplification capability of the replicons was evaluated *in vitro* in BHK cells (Baby Hamster Kidney) transfected (by electroporation) with 200 ng of each RNA to test, or with the same amount of a control RNA of known potency (STD). An anti-double strand RNA antibody was used to detect the percentage of cells positive for a replicating RNA by flow cytometry (Figure 12, c). The frequencies of $dsRNA^+$ BHK cells after transfection with SAM (GM-CSF), or SAM (mutGM-CSF),

or SAM (NP) or SAM (OVA) were even higher than that obtained with the STD, indicating that the new replicons self-amplified appropriately.

a)

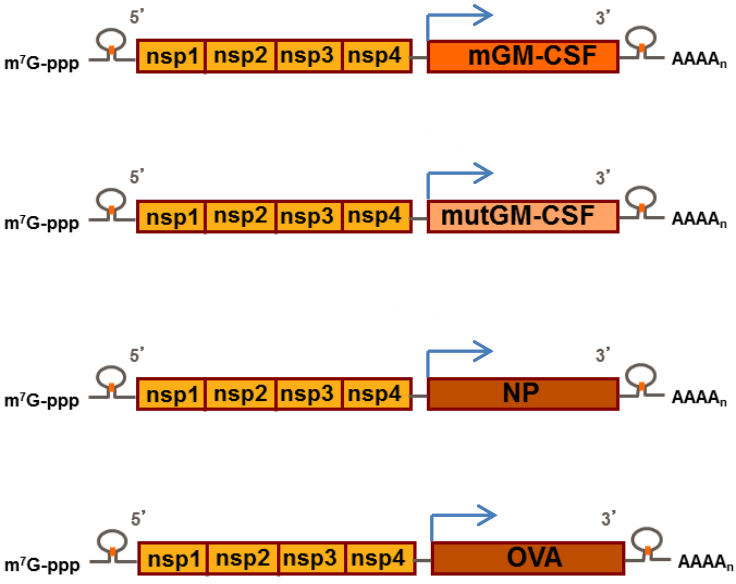

b)

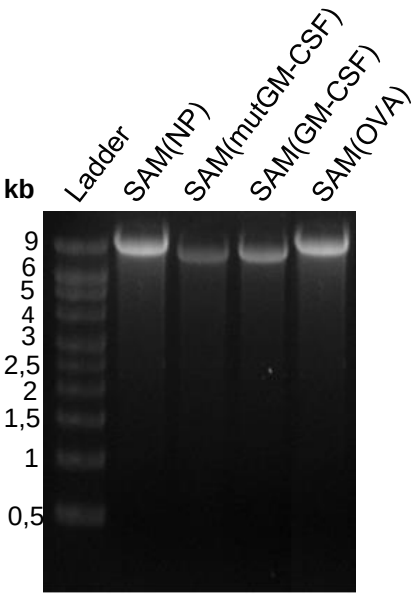

c)

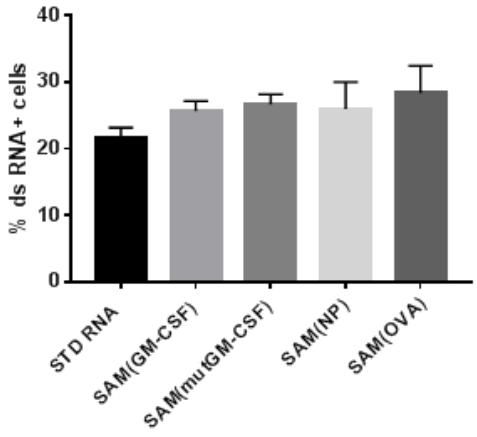

Figure 12
Schematic representation of self-amplifying RNA vectors and their characterization *in vitro*

(a) SAM(GM-CSF), SAM(mutGM-CSF),SAM(NP) and SAM(OVA) constructs, derived from an alphavirus genome, contain a 5' cap, four nonstructural genes (nsp1-4), a 26S subgenomic promoter (blue arrow), the vaccine antigen and a 3' polyadenylated tail.
(b) The integrity of the *in vitro* synthesized RNAs was confirmed by electrophoresis on an agarose gel. RNA ladder (lane 1), RNA after (lane 2) the capping reaction.
(c) Self-amplification capability of SAM vectors was assessed by flow cytometry. The graph shows the percentage of cells containing replicating SAM vectors ($dsRNA^+$ cells).

To evaluate antigen expression, BHK cells were further transfected with 1 µg of each replicon; cell lysates and supernatants were analyzed by Western Blot (Figure 13, a and b) for the expression of OVA, GM-CSF and mutGM-CSF, respectively, while NP expression was evaluated by flow cytometry (Figure 13, d). GM-CSF and mutGM-CSF were detected in the supernatant by using an anti GM-CSF antibody. Both proteins appear as 3 bands, one of the expected molecular weight of 14 kDa, as the positive control (commercial recombinant protein produced in *E. coli*), and the other 2 of higher molecular weight (about 18 and 24 kDa). GM-CSF is a highly glycosylated protein (2 N-glycosylation sites and 2 O-glycosylation sites); to verify whether the higher molecular weight bands were due to N-glycosylation, the protein from the supernatant was treated with PNGaseF for 1h at 37°. After the treatment, the highest molecular weight bands disappear, confirming the correct glycosylation pattern (Figure 13, c). The truncated form of OVA protein was detected in the cell lysate by using an anti-OVA antibody. The protein appears as a band of the expected molecular weight of 40 kDa.

For NP protein, an anti-NP FITC conjugated antibody was used to detect NP by flow cytometry. The percentage of NP expressing cells was comparable to that of a Standard SAM NP of known potency, and correlated to the % of $dsRNA^+$ cells.

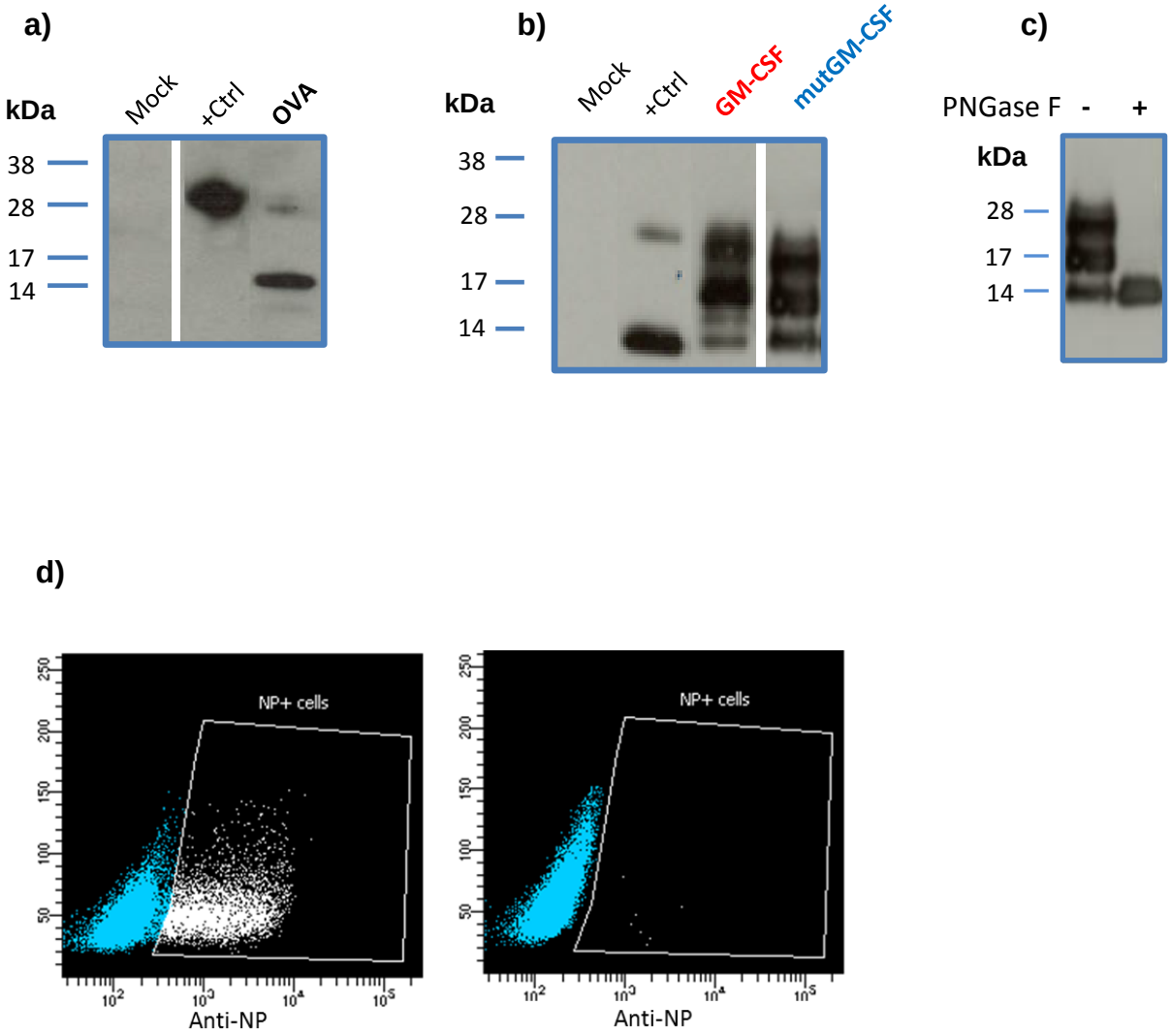

Figure 13
Replicons efficiently express the target antigens.

Efficiency of antigen expression by BHK cells transfected with synthesized RNAs was evaluated by Western blotting (a, b, c) and flow cytometry (d).

Western blot analysis with anti-GM-CSF antibody of supernatants from BHK cells mock transfected or transfected with a SAM(GM-CSF) or SAM(mutGM-CSF) vector. A commercial mouse GM-CSF protein was used as positive control. (c) Western blot analysis of GM-CSF protein from supernatant of BHK cells transfected by SAM GM-CSF, before and after treatment with PNGase F. (d) Flow cytometry analysis of SAM(NP) (left) or mock (right) transfected BHK cells after intracellular staining with anti-NP FITC conjugated antibody.

In vitro biological characterization of GM-CSF and mutGM-CSF

In order to characterize the biological activity of GM-CSF and mutGM-CSF, the coding sequences of both molecules were cloned into a pCMV plasmid with a 6-His tag at the C-terminus. Expi 293 T cells were transfected with the plasmids and 48 hours after transfection, expression of the recombinant proteins was detected in cell supernatants by Western Blot analysis. The proteins were then purified from supernatants via Ni^{2+}-NTA columns and analyzed by SDS PAGE (Figure 14).

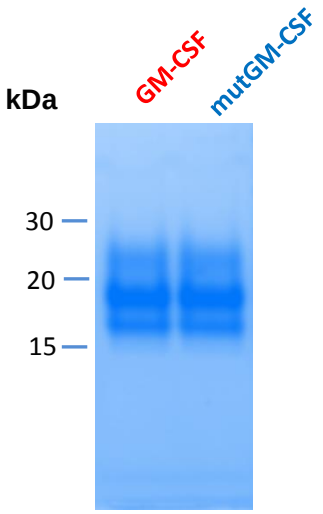

Figure 14

Purification of GM-CSF and mutGM-CSF expressed from Expi 293 T cells for in vitro characterization

SDS-PAGE of GM-CSF and mutGM-CSF purified from supernatants of Expi 293 T cells.

Bone marrow derived monocytes (BMDM) can be differentiated into immature DCs by co-culture with GM-CSF. The ability of the purified GM-CSF to generate Dendritic cells from BMDM was compared to a commercial, recombinant form of GM-CSF used as positive control (Miltenyi). After 8 days of culture, BM derived cells were analyzed by FACS to evaluate the % of $CD11c^{+}/Gr1^{-}$ and $CD11c^{+}/CD80^{+}$ cells. Recombinant GM-CSF and the purified His tagged GM-CSF were equally efficient in generating DCs from BMDM (Figure 15). The positive

control was able to induce 68% of $CD11c^+/Gr1^-$ cells and 62 % of $CD11c^+/CD80^+$ cells, the his-tagged GM-CSF induced 70% of $CD11c^+/Gr1^-$ cells and 74 % of $CD11c^+/CD80^+$ cells). On the contrary, BMDM in the presence of the mutant form of GM-CSF died after 3 days, indicating that it was not biologically active; in fact, in the absence of a specific stimulus of survival and growth, the primary cells died.

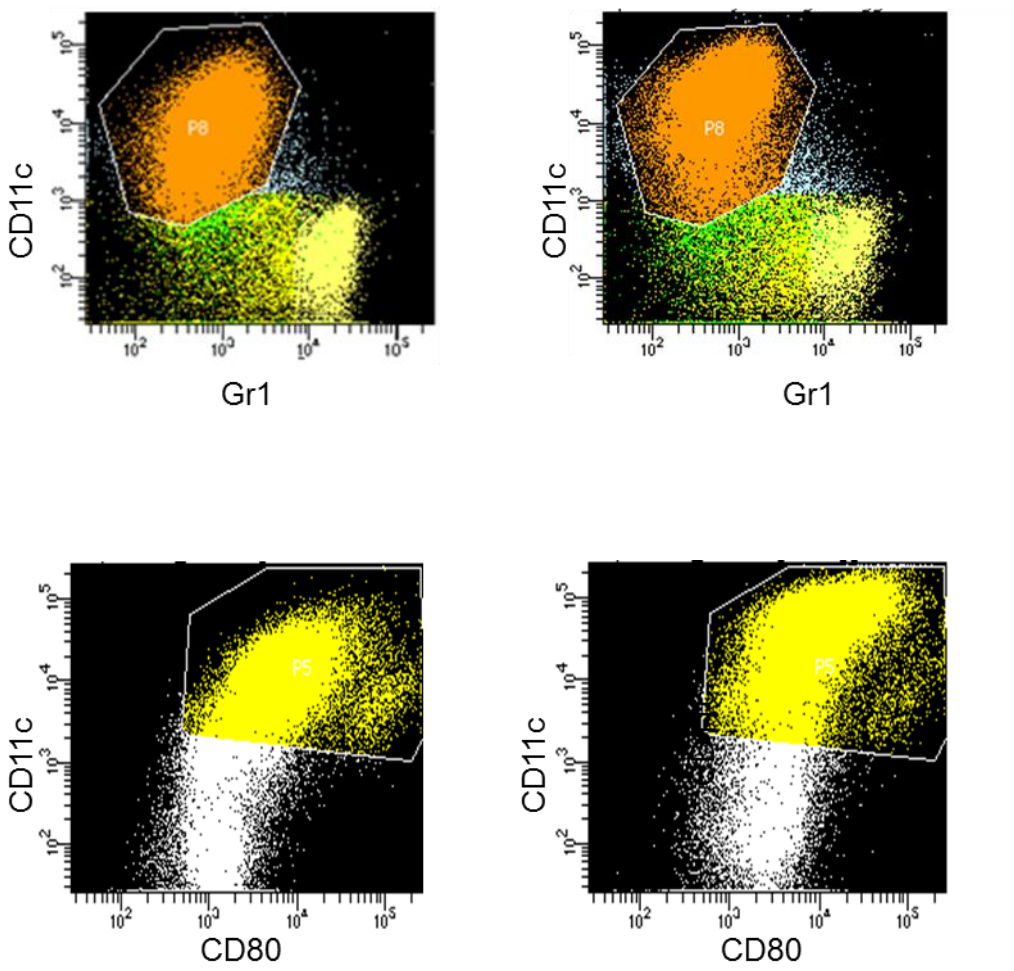

Figure 15
Ability of GM-CSF to generate DCs from BMDM

The graphs show the percentage of differentiated DCs after 8 days in culture with GM-CSF (right panels) or a recombinant GM-CSF (left panels). Differentiated DCs were identified as $CD11c^+/Gr1^-$ cells or $CD11c^+/CD80^+$.

Characterization of CNE formulation

For the *in vivo* studies, the cationic nanoemulsion (CNE) was selected as non-viral delivery system, in particular SAM replicons were formulated with CNE56 [25] in a 1:1 ratio. Each RNA was formulated independently with CNE56 and then the formulated RNAs where mixed when indicated. In this way each RNA can be characterized singularly. Mean particle size and polydispersity were measured by dynamic light scattering for SAM(GM-CSF)/CNE, SAM(mutGM-CSF)/CNE, SAM(NP)/CNE and SAM(OVA)/CNE. Z-average diameters ranged from 133 to 137 nm with a polydispersity index of approximately 0,120 (Figure 16). The formulated SAM were also tested for pH and osmolality; the pH ranged between 6.5 and 7 and osmolality was around 360 mOsm for all the formulations. The analyzed critical quality attributes, included pH, osmolality, particle size and RNA integrity, were all in compliance with the specifications and within acceptance ranges.

RNA integrity after isopropanol extraction from CNE56 was evaluated by 1% agarose gel electrophoresis. The extracted RNAs show no products of degradation (Figure 17).

Formulation	Z-average diameter (nm)	PolyDispersity Index
SAM (GM-CSF)	137	0.126
SAM (mutGM-CSF)	134	0.123
SAM (NP)	135.5	0.120
SAM (OVA)	133.2	0.124

Figure 16
Characterization of SAM/CNE56 formulations

Particle size (Z-average diameter) and polydispersity index were evaluated for each RNA/CNE formulation.

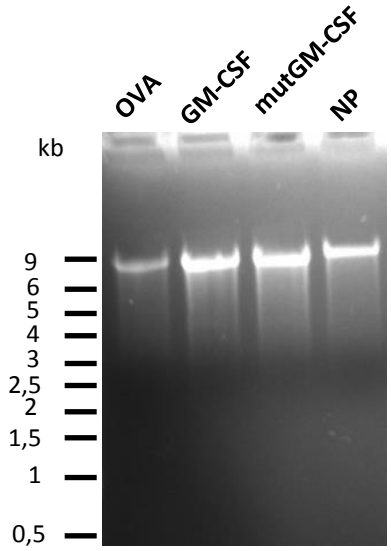

Figure 17
Evaluation of the integrity of SAMs after extraction from CNE56

Agarose gel electrophoresis showing the integrity of the 4 different RNAs after extraction from CNE56.

In vivo recruitment of immune cells at the injection site and in the draining lymph nodes after SAM immunization

The mechanism of action of SAM vaccines is characterized by a cellular infiltrate in the muscle after immunization. To study whether SAM(GM-CSF) was able to increase the recruitment of immune cells *in vivo*, mice were immunized with different SAM combinations and cells from muscles and draining lymph nodes from the differently treated mice were analyzed by flow cytometry.

In a first set-up experiment, mice were immunized with SAM(OVA) + SAM(GM-CSF) while control mice were immunized with SAM(OVA) + SAM(GFP): it is known that CNE per se is able to induce cell recruitment [25], for this reason SAM(GFP) was added to SAM(OVA) in the negative control group as unrelated RNA, in order to administer the same dose of total formulated RNA to the different treatment groups. Immune cell recruitment was assessed from 3 hours to 3 days after the immunization in quadriceps muscles and inguinal draining lymph nodes.

Single cell suspensions were stained with a variety of antibodies to lineage and activation markers followed by flow cytometry. Mice immunized with SAM(GM-CSF) showed a significant increase in the number of immune cells that progressed from day 2 to day 3. In particular, monocytes, macrophages, eosinophils and dendritic cells are the populations that show a high increase (Figure 18, a). While for the control group the peak of recruitment was observed at day 2 and started to decrease at day 3, for mice immunized with SAM(OVA) + SAM(GM-CSF) the recruitment was still raising 3 days after administration.

Based on these results, a second experiment was performed in order to assess the recruitment at longer time points, with 25 days after the immunization as the last time-point evaluated. In this experiment, SAM(GFP) was replaced by SAM(mutGM-CSF), a more appropriate negative control: mice were immunized with SAM(OVA) + SAM(mutGM-CSF) or SAM(OVA) + SAM(GM-CSF). Immune cells infiltration was assessed at different time points after the immunization. At day 3, 4 and 7 after the immunization, mice immunized with SAM(OVA) + SAM(GM-CSF) showed a stronger cellular infiltrate compared to the group immunized with SAM(OVA) + SAM (mutGM-CSF) (Figure 18, b) . In particular, despite the number of infiltrating cells were different in the two groups, the cellular composition did not differ significantly.

There was an increase of monocytes, macrophages and dendritic cells at day 2 in both groups, but while in the group of mice that received mutGM-CSF the recruitment of these cells stopped and the numbers went down, in mice treated with GM-CSF the recruitment went on until day 4. The increased number of dendritic cells, macrophages, and monocytes in mice immunized with SAM(OVA) + SAM (GM-CSF) show a peak at day 4 and then start to decrease. At day 7, all cell number returned to base line level, except for dendritic cells that are still present in the muscle in higher number compared to the control group. At 10 and 24 days after injection, cell numbers were comparable to that of naïve mice. The same effect was observed when mice were immunized with SAM(NP) instead of SAM(OVA) (Figure 18,c). From figure 18, it is clear that the majority of cells recruited were the APCs: a detailed analysis of the APCs subpopulation showed that macrophages and mDCs were recruited at day 3 and 4 in all the experiments in the groups immunized with SAM(GM-CSF) + SAM(NP) or OVA, while neutrophils and monocytes did not show an increase (Figure 19).

a)

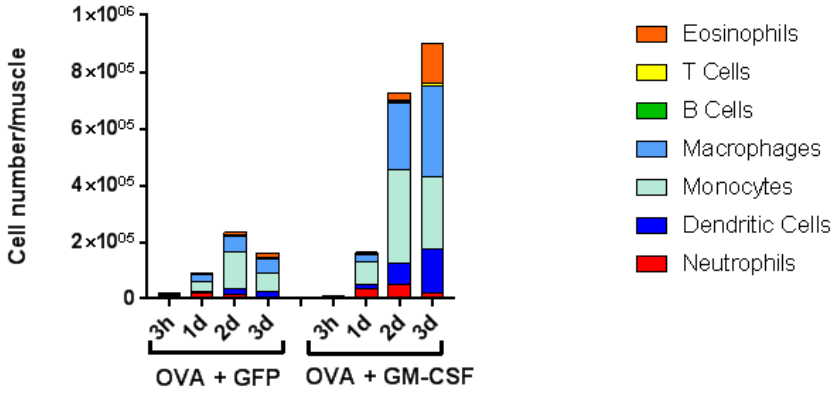
Cell number/muscle
1x10^06
8x10^05
6x10^05
4x10^05
2x10^05
0
3h
1d
2d
3d
OVA + GFP
OVA + GM-CSF
Eosinophils
T Cells
B Cells
Macrophages
Monocytes
Dendritic Cells
Neutrophils

b)

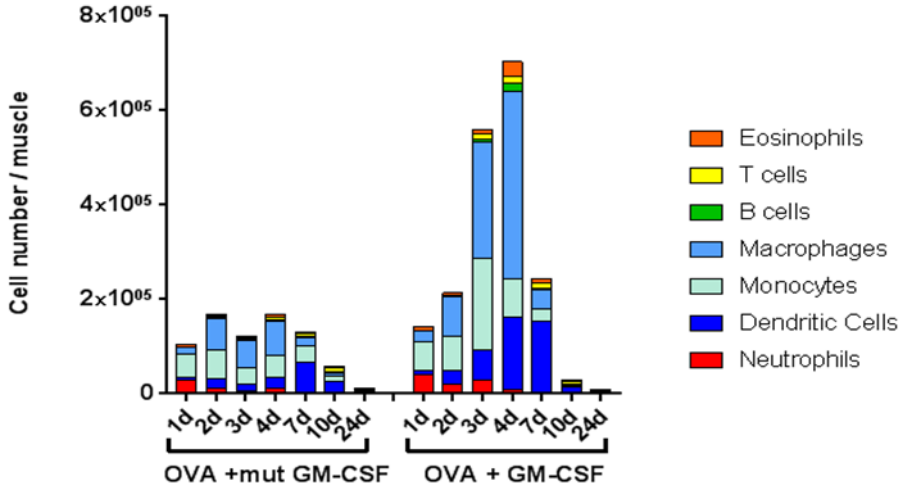
Cell number / muscle
8x10^05
6x10^05
4x10^05
2x10^05
0
1d
2d
3d
4d
7d
10d
24d
OVA +mut GM-CSF
OVA + GM-CSF
Eosinophils
T cells
B cells
Macrophages
Monocytes
Dendritic Cells
Neutrophils

c)

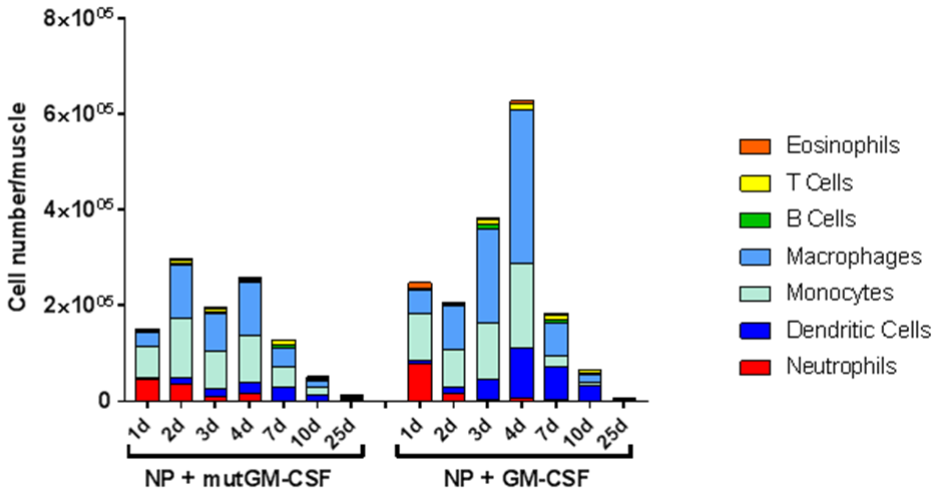

Figure 18

Characterization of cell recruitment in quadriceps muscles following SAM immunization

Quadriceps muscles, both left and right, (n=4) were collected at different time points after the immunization to evaluate cellular composition. Bars represent the total number of cells recruited into the muscles, and colors indicate the different cell types; a) mice immunized i.m. with 1.5 µg SAM(OVA) + 1.5 µg SAM(GFP) or with 1,5 µg SAM(OVA)+ 1.5 µg SAM(GM-CSF); b) mice immunized i.m. with 1.5 µg SAM(OVA) + 1.5 µg SAM(mutGM-CSF) or with 1,5 µg SAM(OVA)+ 1.5 µg SAM(GM-CSF); c) mice immunized i.m. with 1,5 µg SAM(NP)+ 1.5 µg SAM(mutGM-CSF) or with 1,5 µg SAM(NP)+ 1.5 µg SAM(mutGM-CSF)

a)

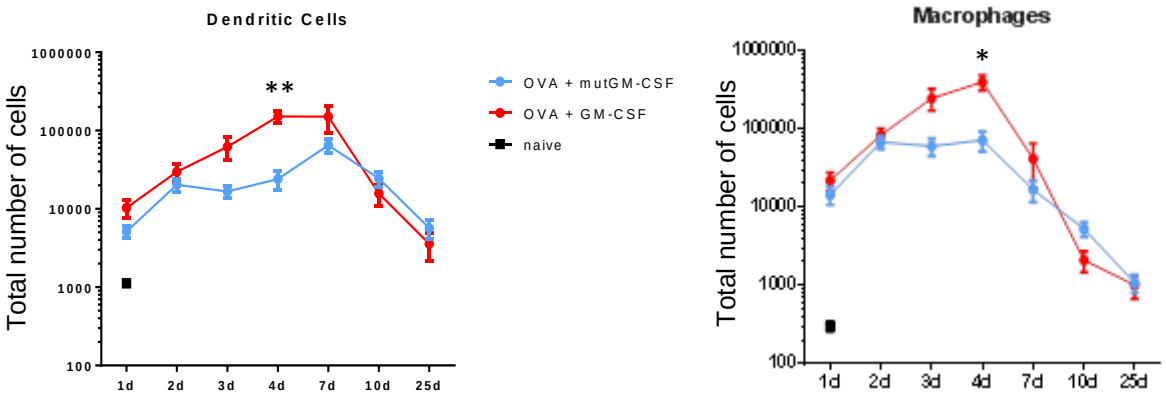

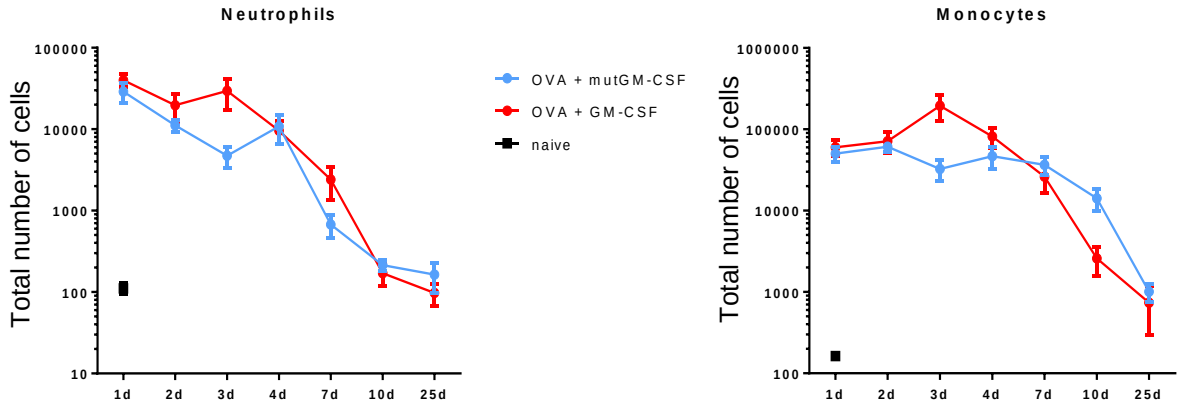
Neutrophils
Monocytes
Total number of cells
1000000
100000
10000
1000
100
10
1d
2d
3d
4d
7d
10d
25d
OVA + mutGM-CSF
OVA + GM-CSF
naive

b)

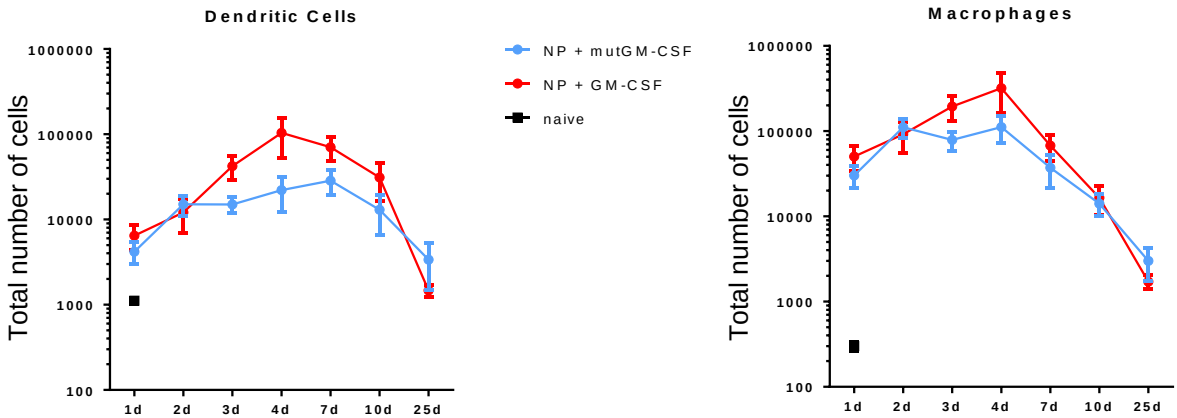
Dendritic Cells
Macrophages
Total number of cells
1000000
100000
10000
1000
100
1d
2d
3d
4d
7d
10d
25d
NP + mutGM-CSF
NP + GM-CSF
naive

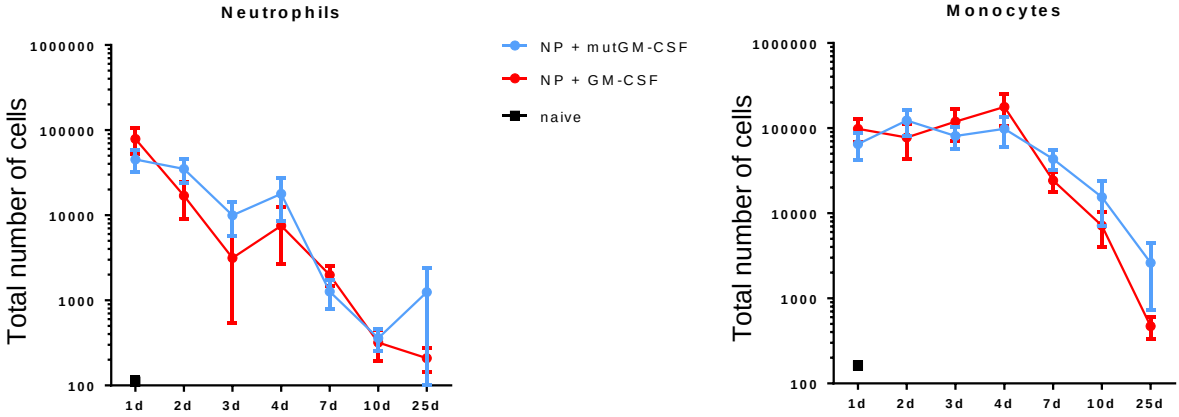
Neutrophils
Monocytes
Total number of cells
1000000
100000
10000
1000
100
1d
2d
3d
4d
7d
10d
25d
NP + mutGM-CSF
NP + GM-CSF
naive

Figure 19
Kinetic of the recruitment of inflammatory cells in quadriceps muscles

Kinetic of neutrophils, monocytes, macrophages, and DCs are indicated for each experimental group; a) mice immunized with SAM(OVA) + SAM(mutGM-CSF) or with SAM(OVA)+ SAM(GM-CSF); b) mice immunized with SAM(NP)+ SAM(mutGM-CSF) or with SAM(NP)+ SAM(mutGM-CSF). Statistical analysis was performed using the Mann-Whitney U test: * $p < 0.05$; ** $p < 0.01$.

Cell recruitment was analyzed also at the level of the inguinal draining lymph nodes of the immunized mice.

Differently from what observed in the injection site, no significative difference was observed between the immunization groups in total number of cells recruited in the inguinal draining lymph nodes, regardless of the model antigen used (Figure 20 a, b and c). A detailed analysis of cell populations revealed a statistically significant increase in the number of monocytes recruited at day 3 for SAM(NP) and at day 4 for SAM(OVA) in mice injected with SAM(GM-CSF) in comparison with mice injected with SAM(mutGM-CSF) (Figure 21 a and b).

a)

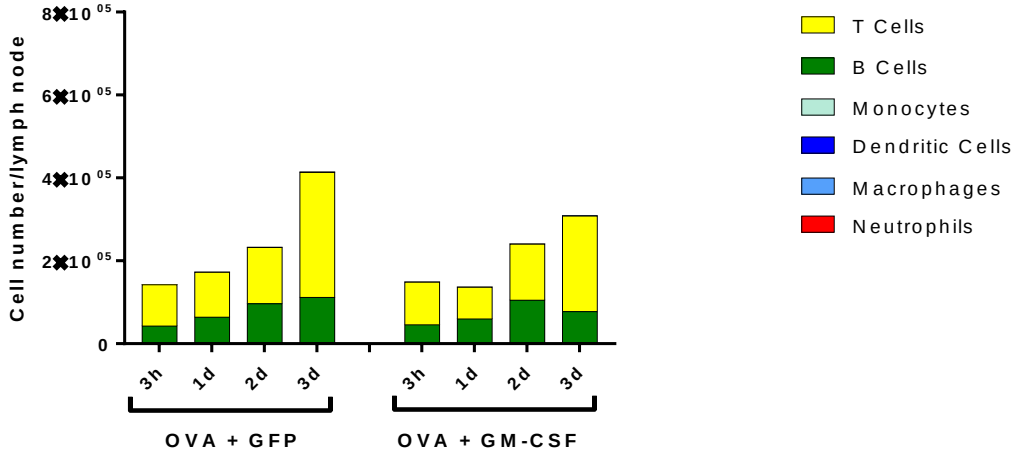
Cell number/lymph node
8✖10 05
6✖10 05
4✖10 05
2✖10 05
0
3h
1d
2d
3d
OVA + GFP
OVA + GM-CSF
T Cells
B Cells
Monocytes
Dendritic Cells
Macrophages
Neutrophils

b)

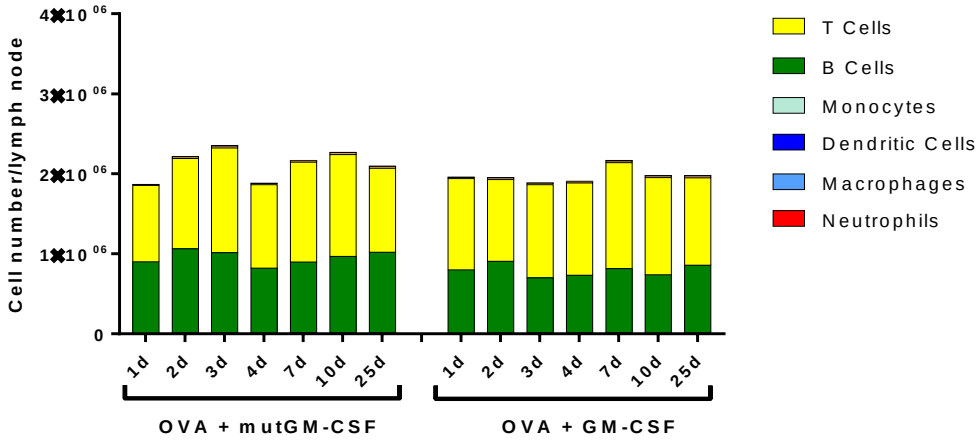
Cell number/lymph node
4✖10 06
3✖10 06
2✖10 06
1✖10 06
0
1d
2d
3d
4d
7d
10d
25d
OVA + mutGM-CSF
OVA + GM-CSF
T Cells
B Cells
Monocytes
Dendritic Cells
Macrophages
Neutrophils

c)

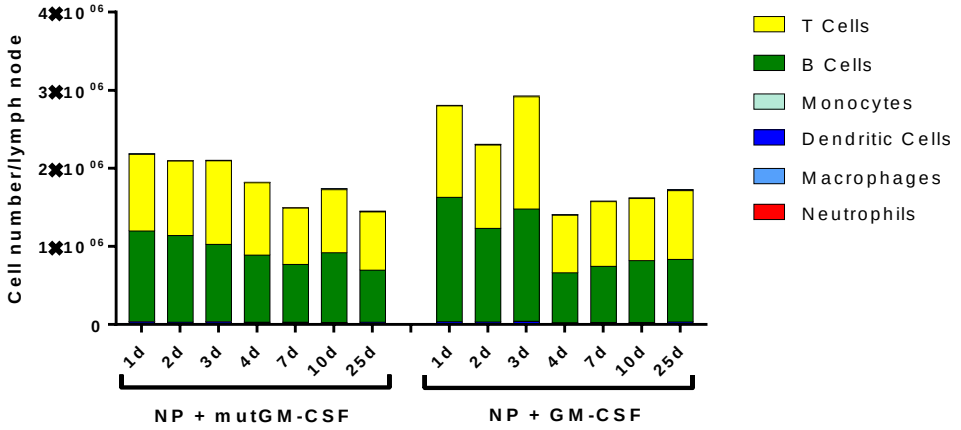
Cell number/lymph node
4✖10 06
3✖10 06
2✖10 06
1✖10 06
0
1d
2d
3d
4d
7d
10d
25d
NP + mutGM-CSF
NP + GM-CSF
T Cells
B Cells
Monocytes
Dendritic Cells
Macrophages
Neutrophils

Figure 20

Characterization of cell recruitment in draining lymph nodes following SAM immunization

Inguinal draining lymph nodes, both left and right, (n=4) were collected at different time points after the immunization to evaluate cellular composition. (a) Bars represent the total number of cells recruited into the muscles, and colors indicate the different cell types: a) mice immunized i.m. with 1.5 µg SAM(OVA) + 1.5 µg SAM(GFP) or with 1,5 µg SAM(OVA)+ 1.5 µg SAM(GM-CSF); b) mice immunized i.m. with 1.5 µg SAM(OVA) + 1.5 µg SAM(mutGM-CSF) or with 1,5 µg SAM(OVA)+ 1.5 µg SAM(GM-CSF); c) mice immunized with 1,5 µg SAM(NP)+ 1.5 µg SAM(mutGM-CSF) or with 1,5 µg SAM(NP)+ 1.5 µg SAM(mutGM-CSF).

a)

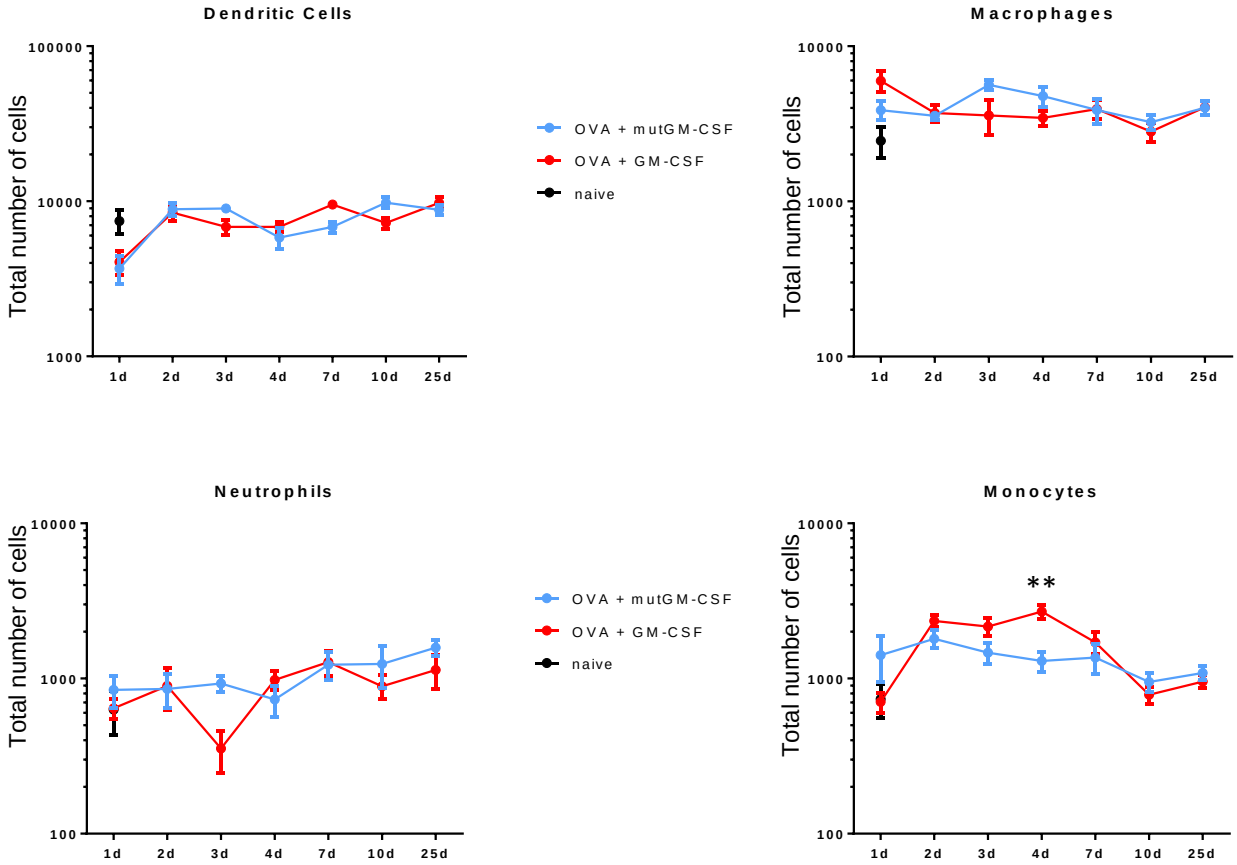

b)

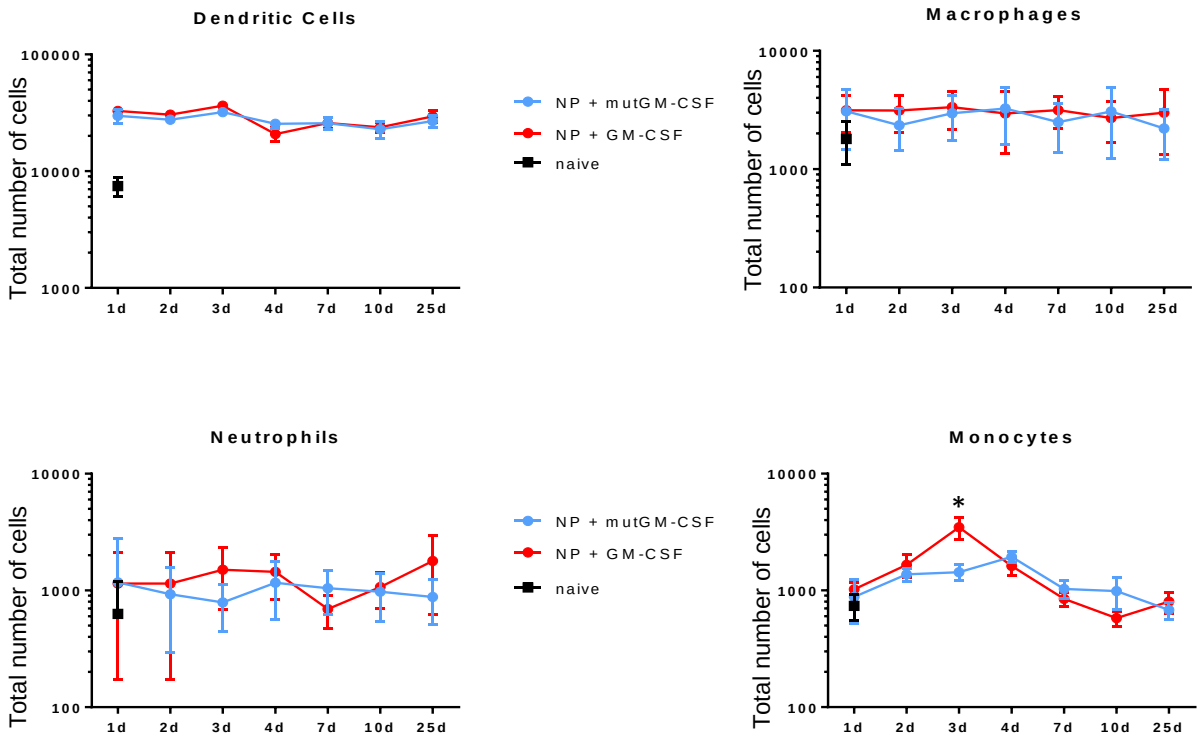

Figure 21
Kinetic of the recruitment of inflammatory cells in draining lymphnodes

Kinetic of neutrophils, monocytes, macrophages, and DCs are indicated for each experimental group; a) mice immunized with SAM(OVA) + SAM(mutGM-CSF) or with SAM(OVA)+ SAM(GM-CSF); b) mice immunized with SAM(NP)+ SAM(mutGM-CSF) or with SAM(NP)+ SAM(mutGM-CSF). Statistical analysis was performed using the Mann-Whitney U test: * $p < 0.05$; ** $p < 0.01$.

Immunogenicity to SAM(OVA) and to SAM(NP)

To assess whether the enhanced recruitment of APCs induced by SAM(GM-CSF) has an impact on immunogenicity, in a first, set-up experiment C57Bl/6 mice were immunized i.m. with 1,5 µg of SAM(OVA) + 1,5 µg SAM(GFP) or with 1,5 µg of

SAM(OVA)+ 1,5 µg SAM(GM-CSF). The immunogenicity to OVA antigen was evaluated both at the cellular and humoral level.

Antigen-specific T-cell response was characterized by intracellular staining (ICS) and flow cytometry (Figure 22 a and b): antigen-specific, cytokine-secreting cells were identified among $CD44^{high}$ $CD8^{+}$ and $CD4^{+}$ T cells following the gating strategy showed in figure 11. 10 days after immunization, splenocytes derived from immunized mice were stimulated *in vitro* either with the MHC class I (H-2Kb)-restricted peptide epitope of ovalbumin $OVA_{257-264}$ peptide, the MHC class II (I-Ad)-restricted peptide epitope of ovalbumin $OVA_{323-339}$ peptide or with the recombinant OVA protein.

OVA-specific CD8+ T-cells frequencies ranged around 0,4% for SAM(OVA)+ SAM(GFP) immunized mice, and 0,7% for mice immunized with SAM(OVA)+ SAM(GM-CSF)(Figure 22, a). The majority of OVA-specific CD8+ T-cells were IFN-γ^{+} or IFN-γ^{+}/TNFα^{+} in both treatment groups; SAM(GM-CSF) was therefore able to induce an increase in the total number of CD8+ T-cells but did not change the quality of the response. OVA-specific CD4+ T-cells were not detectable, independently from the stimulus used ($OVA_{323-339}$ peptide or recombinant OVA protein), in none of the immunization groups (Figure 22, b).

OVA-specific antibody titers were analyzed by ELISA: no IgG were detectable in sera collected 3 weeks after immunization in none of the immunization groups (data not shown); this data were in line with the CD4+ T-cells response results.

a) **b)**

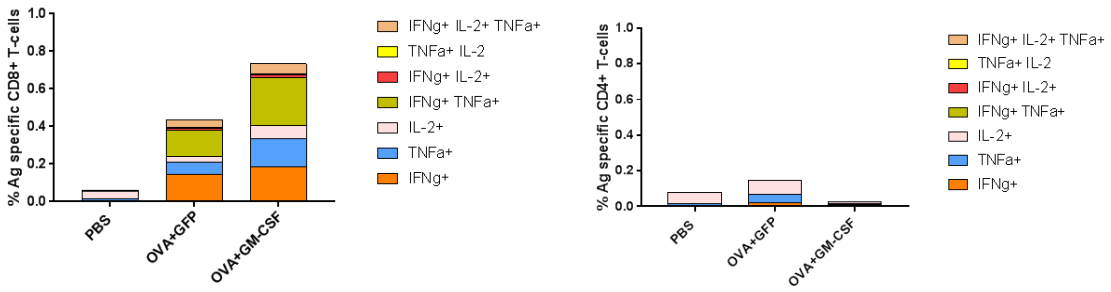

c) **d)**

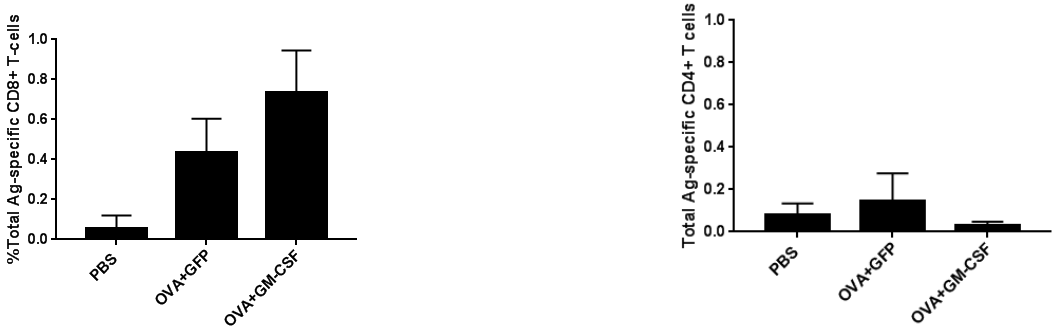

Figure 22

T-cell responses induced by SAM formulations

(a - b) C57Bl/6 mice were immunized i.m. once with 1,5 µg of SAM(OVA)+ SAM(GFP), or with SAM(OVA)+SAM(GM-CSF). Ten days after the immunization, 4 mice per group were sacrificed, an intracellular staining and FACS analysis were performed on splenocytes stimulated *in vitro* with the $OVA_{147-155}$ peptide (a) or with the recombinant OVA protein (b). Graphs show the cumulative frequency of antigen (Ag)-specific, cytokine-secreting $CD8^+$ (a) or $CD4^+$ (b) T cells, and the color code indicates the different type of cytokine produced by the respective cells, as indicated. In c) and d) the frequency of total Ag-specific cytokine secreting $CD8^+$ T cells and $CD4^+$ T cells, respectively.

The same kind of analysis was performed to assess the impact of SAM (GM-CSF) on NP immunogenicity. C57Bl/6 mice were immunized i.m. either with 1,5 µg of SAM(NP), or with 1,5 µg of SAM(NP) + 1,5 µg SAM(mutGM-CSF) or with 1,5 µg of SAM(NP) + 1,5 µg SAM(GM-CSF). The antigen-specific T-cell response was assessed 10 days after the immunization: splenocytes were stimulated *in vitro* with the MHC class I-restricted peptide epitope $NP_{147-155}$ (Figure 23, a) or with recombinant NP protein (Figure 23, b).

The frequencies of NP-specific $CD8^+$ T-cells ranged around 0.4 % of total $CD8^+$ T-cells for SAM(NP) and SAM(NP)+ SAM(mutGM-CSF) immunized mice, around 0.8% in SAM(NP)+SAM(GM-CSF) immunized mice. As observed for immunizations performed using OVA as model antigen, the majority of NP-specific $CD8^+$ T-cells were IFN-γ^+ and IFN-γ^+/TNFα^+, characteristic of an effector phenotype.

NP-specific CD4+ T-cells were detectable after one immunization and showed predominantly the Th0 phenotype (IL-2^+/TNFα^+, TNFα^+, and IL-2^+) or the multifunctional Th1 phenotype (IFN-γ^+/IL-2^+/TNFα^+). As shown in figure 23 b, NP-specific $CD4^+$ T-cells induced by SAM(GM-CSF) were slightly but not significantly higher with respect to the other immunization groups.

a)

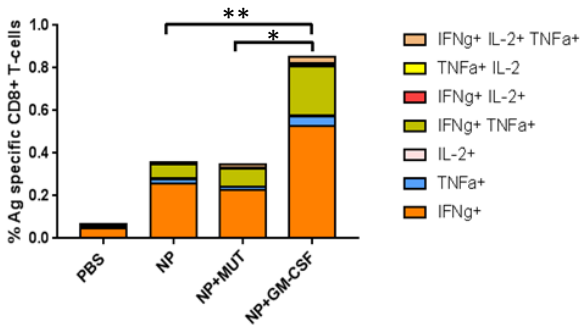

b)

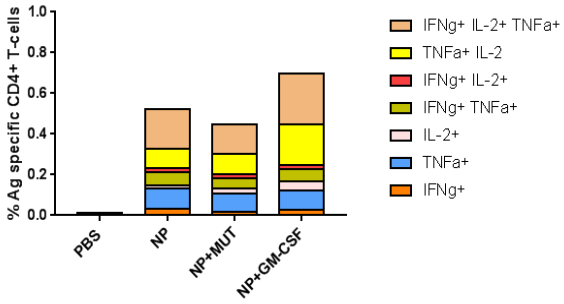

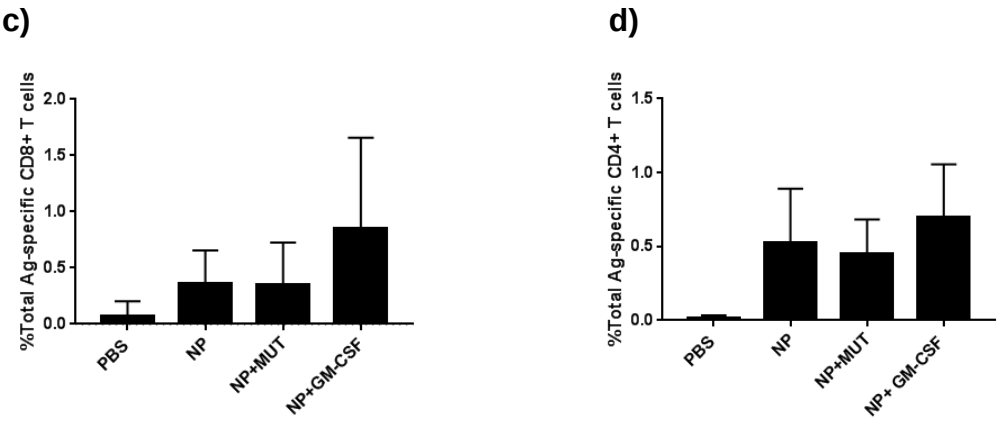

Figure 23
T-cell responses induced by SAM formulations

(a - b) C57Bl/6 mice were immunized i.m. once with 1,5 µg of SAM(NP), or with 1,5 µg of SAM(NP)+ SAM(mutGM-CSF) or with SAM(NP)+SAM(GM-CSF). Ten days after the immunization, 6 mice per group were sacrificed, an intracellular staining and FACS analysis were performed on splenocytes stimulated *in vitro* with the $NP_{147-155}$ peptide (a) or with the recombinant NP protein (b). Graphs show the cumulative frequency of antigen (Ag)-specific, cytokine-secreting $CD8^+$ (a) or $CD4^+$ (b) T cells, and the color code indicates the different type of cytokine produced by the respective cells, as indicated. In c) and d) the frequency of total Ag-specific cytokine secreting $CD8^+$ T cells and $CD4^+$ T cells, respectively. Representative data are the mean ± standard deviation (SD) of 6 mice from each group and were analyzed by Mann-Whitney U test: * $p < 0.05$; ** $p < 0.01$.

The humorale response to NP was evalueted by assessing the presence of NP-specific IgG in the sera of SAM-immunized mice. Mice that received SAM(NP)+SAM(GM-CSF) reached antibody titers comparable to those of mice vaccinated with SAM(NP) only or SAM(NP)+SAM(mutGM-CSF) (Figure 24).

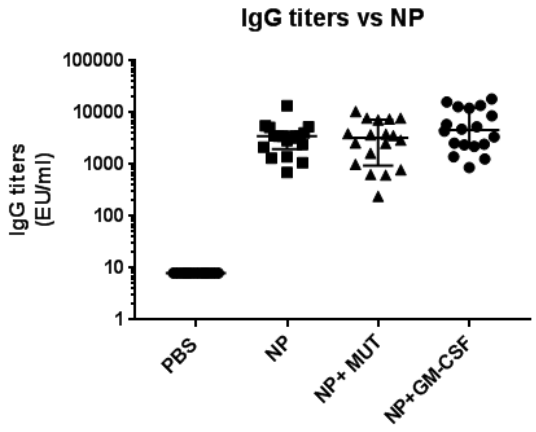

Figure 24
SAM(GM-CSF) has no effect on antigen-specific IgG

Sera samples were collected 3 weeks post 1 immunization to determine NP specific IgG titers by ELISA. Statistical analysis was performed using the Mann-Whitney U test.

SAM (GM-CSF) enhances the cytotoxic activity of CD8 T cells

Finally, we characterized antigen-specific T cells induced by SAM vaccines for cytotoxic activity *in vitro* and *in vivo* (Figure 25).

Antigen-specific T cell cytotoxicity was evaluated by measuring the surface expression of CD107a, as a measure of the degranulation process, upon *in vitro* antigen-stimulation of splenocytes derived from immunized mice. CD107a is a lysosomal membrane protein that is transiently expressed on the T cell surface as a result of the degranulation process and is associated with T cell cytotoxicity. The immunization with SAM(NP) + SAM(GM-CSF) induced a higher frequency of $CD107a^+$ NP-specific CD8 T cells compared to the other treatments. The majority of NP-specific $CD8^+$ T cells were $CD107a^+$ for all the immunization groups (Figure 25, a).

To evaluate the *in vivo* cytotoxic activity of NP-specific CD8 T cells, an equivalent number of splenocytes derived from naïve mice were pulsed with the H2-K^d restricted $NP_{147\text{-}155}$ peptide (and stained with 0.5 µM CFSE) or with an unrelated

OVA $_{257-264}$ peptide (and stained with 10 µM CMTMR). The two population were then mixed and adoptively transferred intravenously in mice immunized with either 1,5 µg of SAM(NP), 1,5 µg of SAM(NP)+ 1,5 µg SAM(mutGM-CSF) or 1,5 µg of SAM(NP) + 1,5 µg SAM(GM-CSF). The percentage of $CFSE^+$ and $CMTMR^+$ cells present in the spleens were measured by flow cytometry 18 hrs after the adoptive transfer. In mice immunized with SAM(NP) or SAM(NP) + SAM (mutGM-CSF), an equal specific lysis of 84% was achieved (Figure 25, b). In the group immunized with 1,5 µg of SAM (NP) + 1,5 µg SAM(GM-CSF), we detected a specific lysis of 98%, statistically significantly higher than the one observed in the other groups. No specific lysis was detected in PBS treated mice confirming the specificity of the cytotoxic activity. These results demonstrated that SAM(GM-CSF) is able to enhance the cytotoxic activity of the induced CD8 T cells *in vivo.*

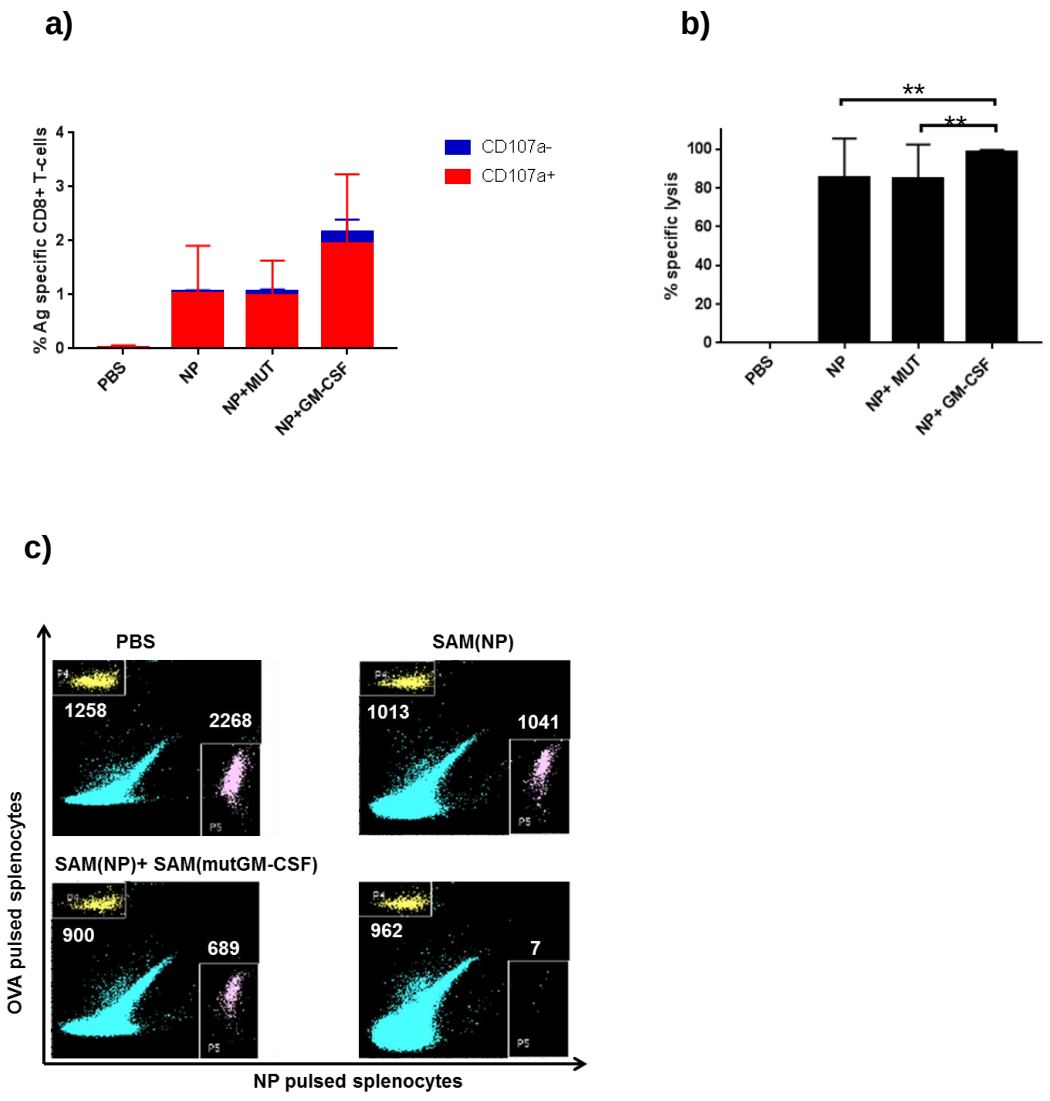

Figure 25
SAM(GM-CSF) increases the cytotoxic activity of NP-specific CD8 T cells *in vitro* and *in vivo*

(a) The surface expression of the CD107a marker was assessed. The bars show the percentage of cytokine secreting CD8 T cells that express (red bars) or not (blue bars) CD107a.

(b) Spleens from mice immunized with SAM(NP) alone or in combination with SAM(mutGM-CSF) or SAM(GM-CSF) were collected 10 days after the first immunization to measure the induction of cytotoxic NP-specific CD8+ T cells by flow cytometry. The graphs show the percentage of NP-specific lysis calculated for each immunization group. Representative data are the mean ± standard deviation (SD) of 6 mice from each group and were analyzed by Mann-Whitney U test: * $p < 0.05$; ** $p < 0.01$. (c) Representative dot plots indicating the numbers of $CMTMR^+$ and $CFSE^+$ cells in each immunization group are shown.

Administering SAM(NP) at the peak of APCs recruitment has no effect on the cellular response

Considering that APCs recruitment at the injection site reaches a peak at day 4 after the immunization, we wondered whether administering the SAM(NP) at the peak of recruitment could have a beneficial effect on the CD8 T cell response. For this purpose, mice were first immunized with SAM(mutGM-CSF), with SAM(GM-CSF), or PBS 3 days before the administration of SAM(NP). 10 days after the administration of the antigen, intracellular cytokine staining was performed. The effect of increase in the CD8 T cell response observed when SAM(GM-CSF) was co-administered with SAM(NP), was lost when administering SAM(GM-CSF) 3 days before. Indeed all the immunization groups reached the same percentage of CD8 T cells and no increase was observed in the group immunized with SAM(GM-CSF) (Figure 26). We can therefore conclude that SAM(GM-CSF) better exerted its effect when it was co-administered with the antigen.

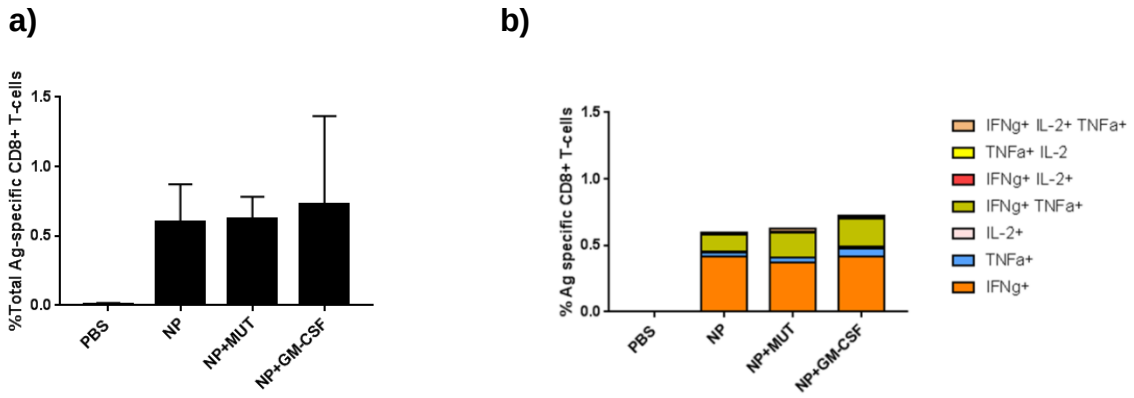

Figure 26

The administration of SAM(GM-CSF) at the peak of APCs recruitment has no effect on the cellular response

C57Bl/6 mice were immunized i.m. with PBS, or 1,5 µg of SAM(mutGM-CSF) or with 1,5 µg of SAM(mutGM-CSF) or with SAM(GM-CSF). 3 days after SAM(NP) was administered to all groups of mice.Ten days after the immunization with SAM (NP), 6 mice per group were sacrificed, an intracellular staining and FACS analysis were performed on splenocytes stimulated *in vitro* with the $NP_{147-155}$ peptide. Graphs show the cumulative frequency of antigen (Ag)-specific, cytokine-secreting $CD8^+$T cells (a), and the color code indicates the different type of cytokine produced by the respective cells, as indicated (b).

Effect of SAM (GM-CSF) treatment in protection against influenza virus challenge

To explore the adjuvant effect of SAM(GM-CSF) on protection to Influenza A Virus, C57Bl/6 mice were immunized with 1.5 µg of SAM(NP), 1.5 µg of SAM(NP)+ 1,5 µg SAM(mutGM-CSF) or 1,5 µg of SAM (NP) + 1,5 µg SAM(GM-CSF), and challenged with 38 $TCID_{50}$ of influenza A/PR/8/34 (H1N1) virus. Animal weight was monitored for 14 days after the infection (Figure 27).

Unexpectedly, the PBS-treated control mice showed a higher survival rate (75%) and a more limited body weight loss at the peak of infection (10%), as compared to prior virus dose finding experiments (LD50, lethal dose 50). One possible explanation is that a change in the anesthesia technique, introduced in our animal

facility shortly prior to the experiments, altered the experimental settings. Thus, the virus needs to be re-titrated with the new infection conditions. The consequence of this low infection level is that mice immunized with the different combinations of SAM(NP) were all protected with a 100% survival rate and a very limited weight loss narrowing the window of experimental readout. Nevertheless, a trend of better fitness was observed for mice immunized with SAM(NP) + SAM(GM-CSF), in two independent experiments.

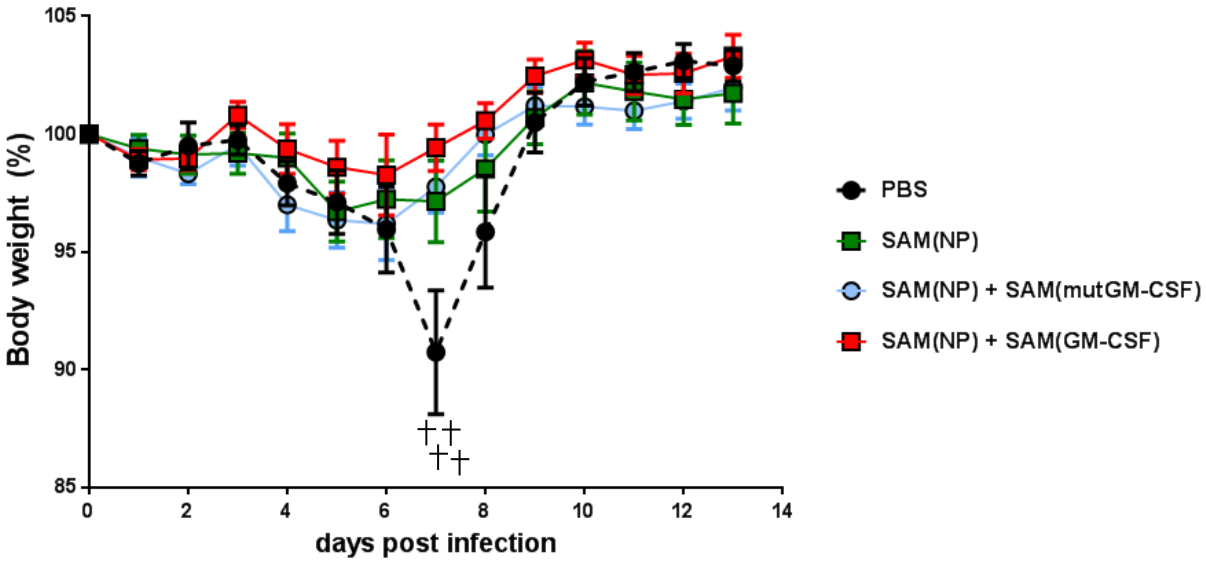

Figure 27

SAM(NP) containing formulations protect mice against lethal influenza challenge

C57Bl/6 mice (16 mice/group) were immunized i.m. with 1,5 µg of SAM(NP),1,5 µg of SAM(NP)+ 1,5 µg of SAM(mutGM-CSF), or with 1,5 µg of SAM(NP)+ 1,5 µg of SAM(GM-CSF). Four weeks after the injection, mice were challenged with 38 $TCID_{50}$/mouse of homologous influenza virus A/PR8/34 (H1N1). Mice were monitored for body weight loss for 14 days post infection and euthanized if the body weight loss was superior than 20%. Graphs show mean of single mice ± SEM.

Reactogenicity analysis

Levels of inflammatory cytokines and body weight were measured to evaluate if SAM (GM-CSF) treatment induced a reactogenic profile. A panel of 23 cytokines (pro-inflammatory and anti-inflammatory) was evaluated in the sera of immunized mice 1, 2, 3, days after the injection. The curve represents the mean of cytokine concentration as pg/ml + SD. We observed no difference in the level of proinflammatory and anti-inflammatory cytokines between mice immunized with SAM(OVA)+ SAM(GFP) and mice treated with SAM(OVA)+ SAM(GM-CSF) (Figure 28). Body weight loss was the parameter of choice as read-out of pain and discomfort or global impairment of health in small rodents [95]. Body weight was monitored in immunized mice along 4 days after the immunization. The mice from both groups did not show any severe body weight loss; on the contrary, they gained weight 2 days after the immunization (Figure 29). To further characterize the reactogenic profile, we wanted to exclude that the administration of SAM(GM-CSF) induces autoantibodies antiGM-CSF. No antibodies anti GM-CSF were detected 3 weeks after the immunization, both for SAM(NP) +SAM(GM-CSF) and for SAM(OVA)+SAM(GM-CSF) immunized mice (Data not shown). We can conclude that SAM(GM-CSF) did not induce a reactogenic profile to be considered with caution.

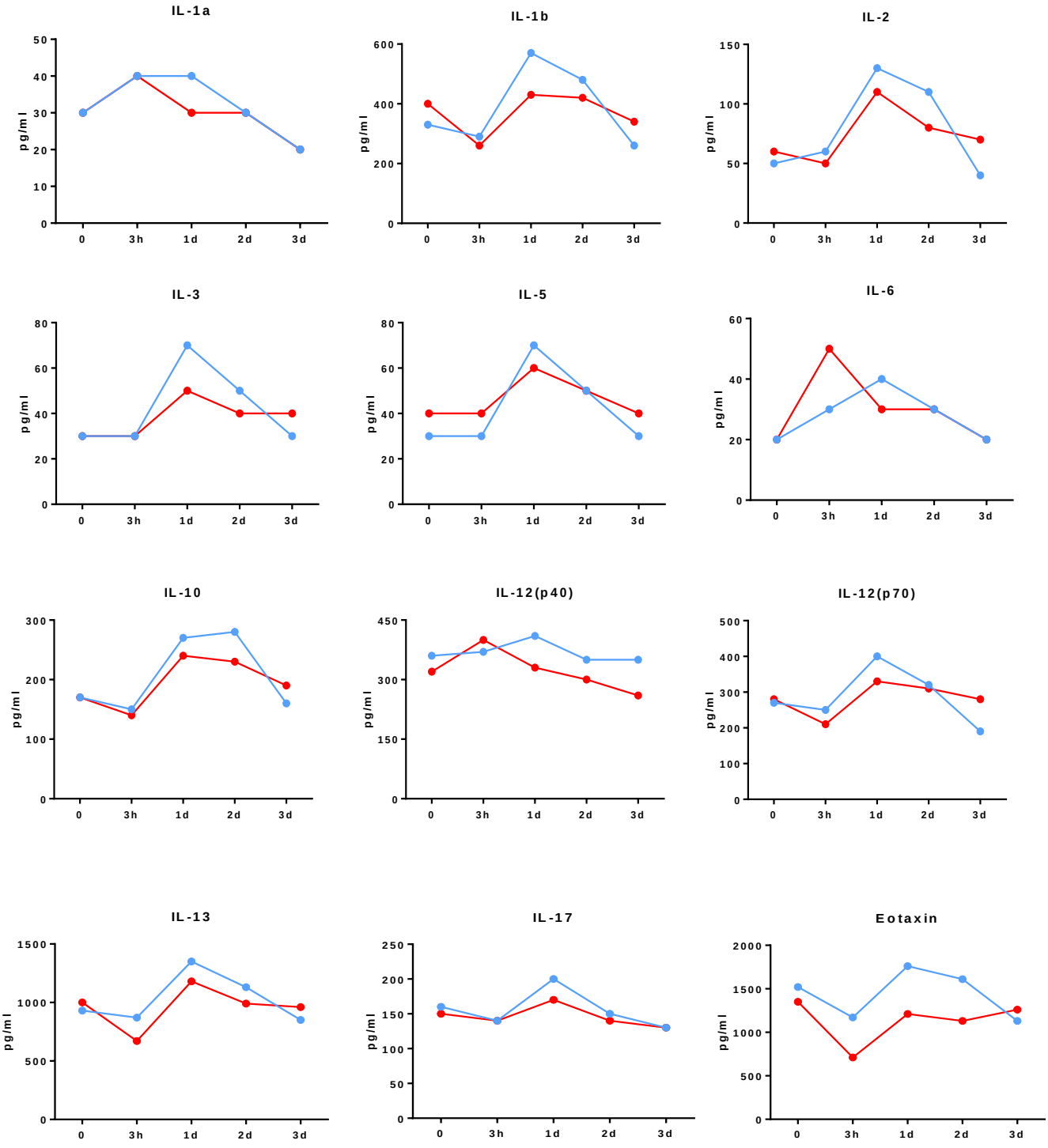
IL-1a
IL-1b
IL-2
IL-3
IL-5
IL-6
IL-10
IL-12(p40)
IL-12(p70)
IL-13
IL-17
Eotaxin
pg/ml
0
3h
1d
2d
3d

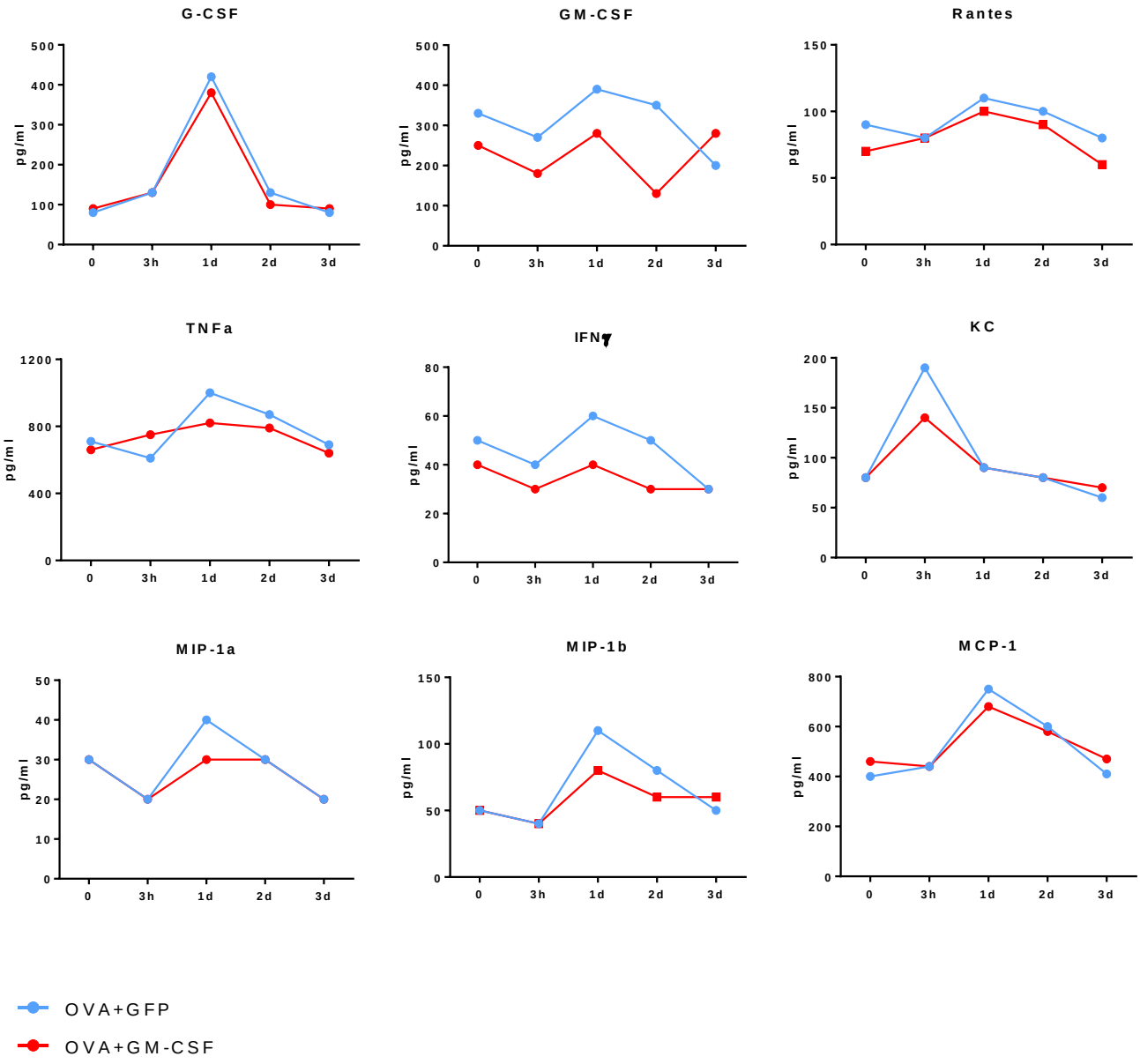

Figure 28
Cytokine evaluation

Mice were immunized with SAM(NP) alone or in combination with mutGM-CSF or GM-CSF. At the indicated time points, sera were evaluated for a panel of cytokine. The curves represent mean of cytokine concentration as pg/ ml + SD.

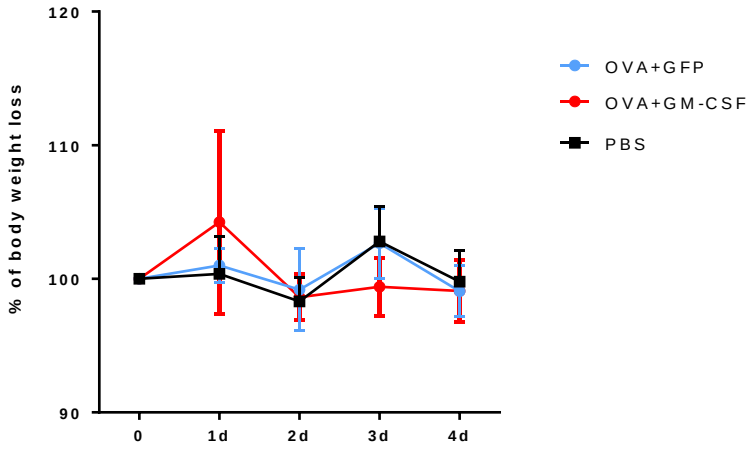

Figure 29
Body weight loss evaluation

Body weight of mice was monitored until day 4 after the immunization. The curves represent the mean+SD of body weight loss for each treatment group.

PART II

Construction and expression of fusion contructs to target DCs

In order to improve presentation of the antigen to T cells, therefore the immune response, we have explored the possibility to target the Antigen to 3 different receptors expressed on CD8+ DCs: DEC205, CLEC 9a and XCR1. To deliver antigen to these molecules, we cloned heavy and light chain variable regions from the monoclonal antibody to DEC205 and CLEC9a and genetically fused OVA with a glycine serine linker, obtaining scFv anti-DEC205-OVA and scFv anti-CLEC9a-OVA respectively. To target XCR1, we cloned the coding sequence for XCL1, the specific ligand for XCR1, and fused to OVA (XCL1-OVA). A scFv anti-Nad A protein was fused to OVA and used as negative control for the experiments as it does not bind to DCs. Alternative fusion constructs to target DCs were obtained by putting OVA at the N terminus of the construct (Figure 30). All the fusion constructs were transfected in Expi293 T cells. Expression and secretion of the constructs was evaluated by WB in supernatants of transfected cells. As shown in figure 31, all the fusion constructs appear on WB at the expected molecular weight in supernatants of transfected cells. The constructs were then purified by Ni-NTA to test them for binding to DCs.

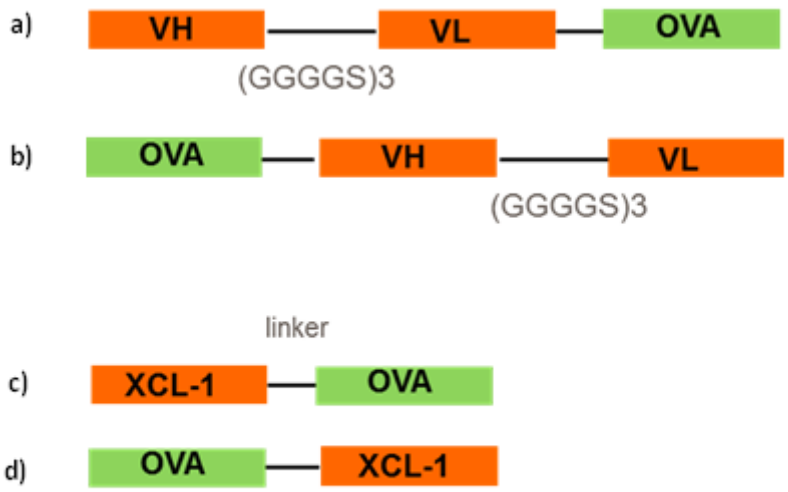

Figure 30

Design of fusion constructs to target DCs

a)Heavy-chain (VH) and light-chain (VL) variable regions of each mAb anti DEC-205 and antiCLEC9a were connected by an interchain linker (GGGGS)3 and cloned in frame upstream of the cDNA for OVA separated by a GSGGGG linker. b) OVA full length cDNA as cloned upstream of the scFv anti-DEC-205 and anti-CLEC9a. c) murine XCL1 cDNA was fused to OVA full length cDNA by a GSGGGG linker. d) OVA full length cDNA was cloned upstream of the XCL1 cDNA.

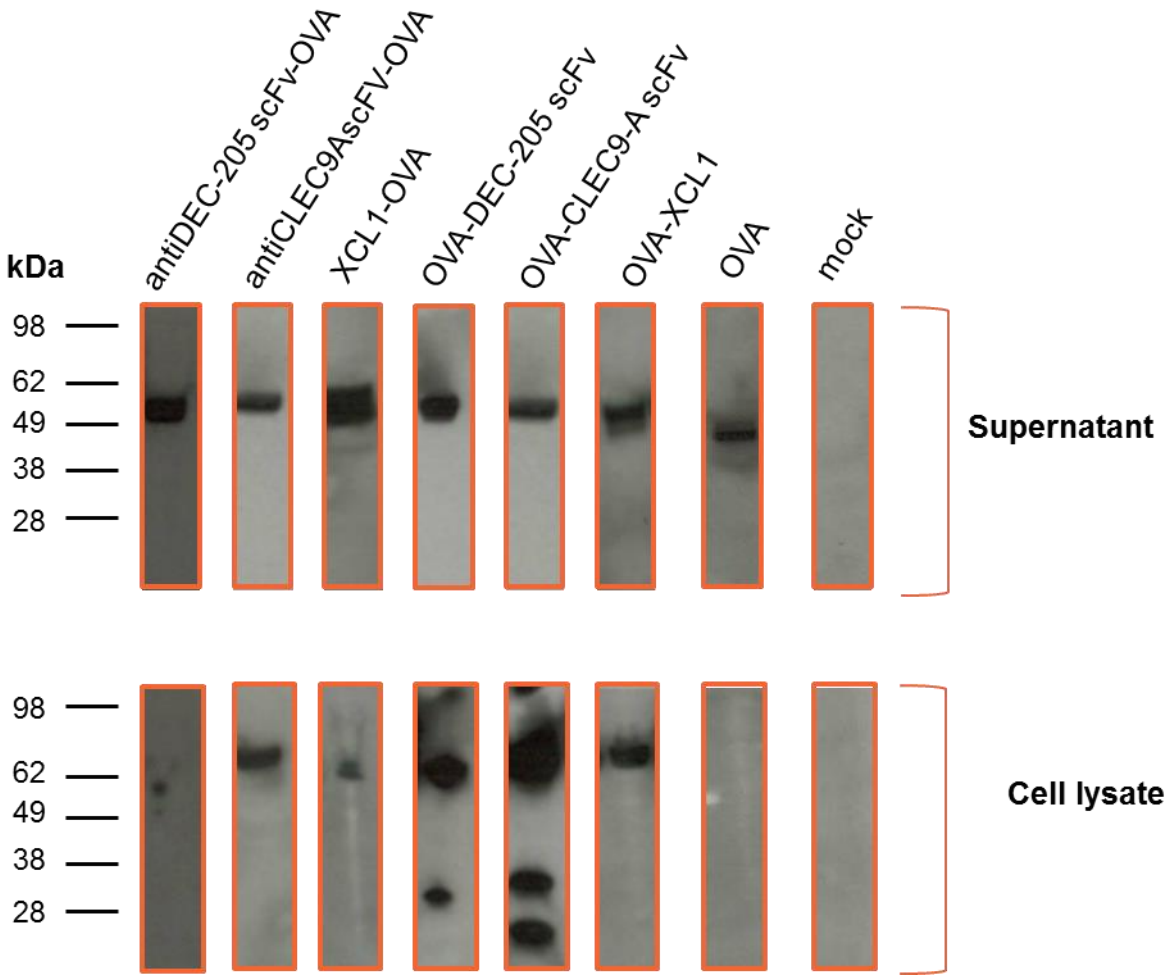

Figure 31
Analysis of the expression of the fusion contructs

Supernatants and cell lysates of Expi 293T cells transfected with expression plasmids for the different fusion constructs or mock transfected were Western blotted using an Ab against OVA.

In vitro targeting of antigen to DCs

To verify that the fusion proteins were able to recognize the specific receptors expressed on target DCs, we measured specific binding to mouse splenocytes incubated with each construct. After the incubation, a secondary antibody to OVA-

FITC conjugated was used to detect OVA-positive DCs, identified as CD11c+/MHCII+/CD8a+. We compared the binding activity of each fusion construct to its alternative form in which the OVA protein is at the N terminus. As shown in figure 32, OVA-scFv anti-DEC205 was able to bind better than scFv-antiDEC205-OVA. The fusion constructs that should target CLEC9a receptors showed a very low binding activity. In particular scFv anti-CLEC9a seemed to be unable to bind the receptor, while OVA-scFv anti-CLEC9a barely binded to DCs.
A higher percentage of OVA positive cells were found when cells were incubated with XCL1-OVA than with OVA-XCL1 (Figure 32). On the basis of this in vitro assay, we selected OVA-scFv(anti-DEC205), XCL1-OVA and OVA-scFv(anti-CLEC9a) as fusion constructs to be cloned in the next future into the SAM backbone and to be tested *in vivo* to evaluate whether they were able to induce an increase in the immunogenicity to OVA antigen. This approach has not been prosecuted because there was no more time to start the immunogenicity studies testing the different constructs.

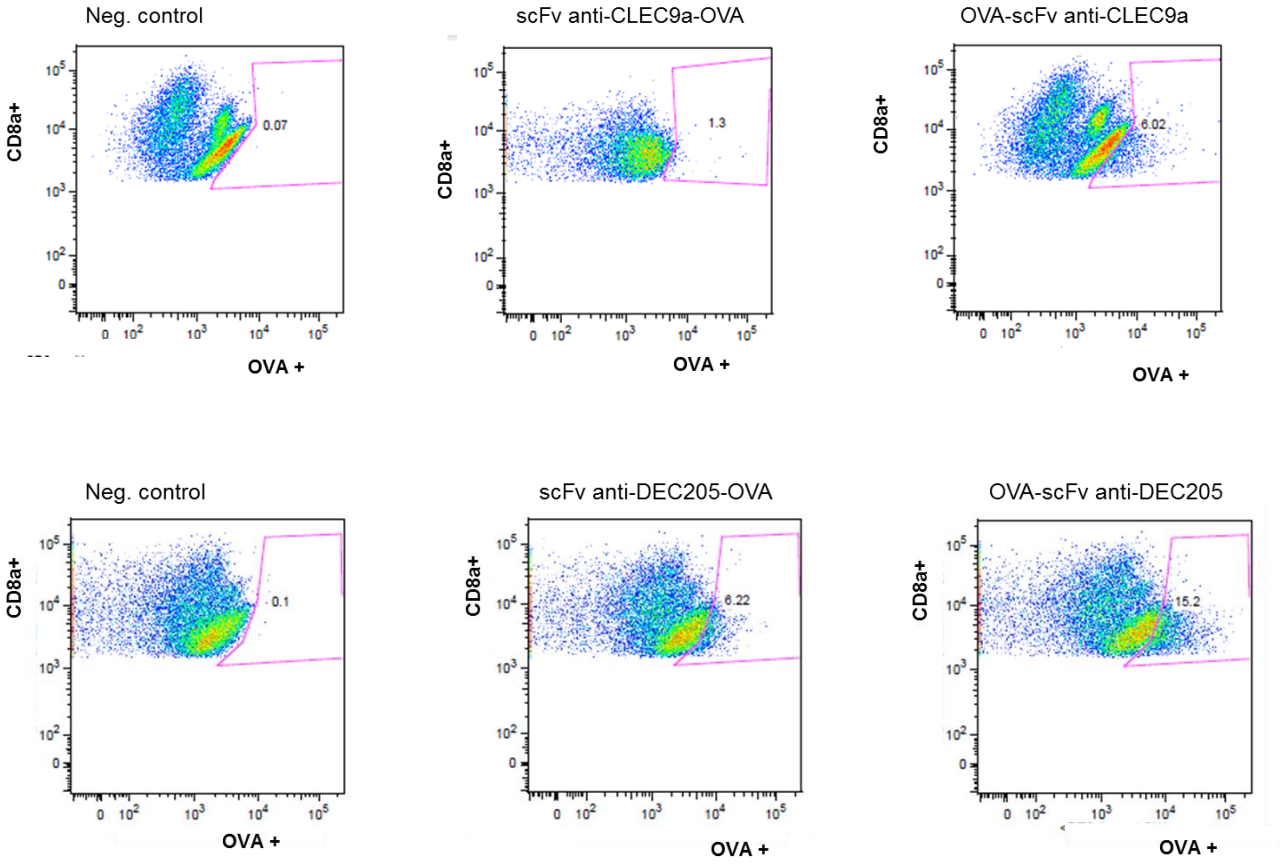

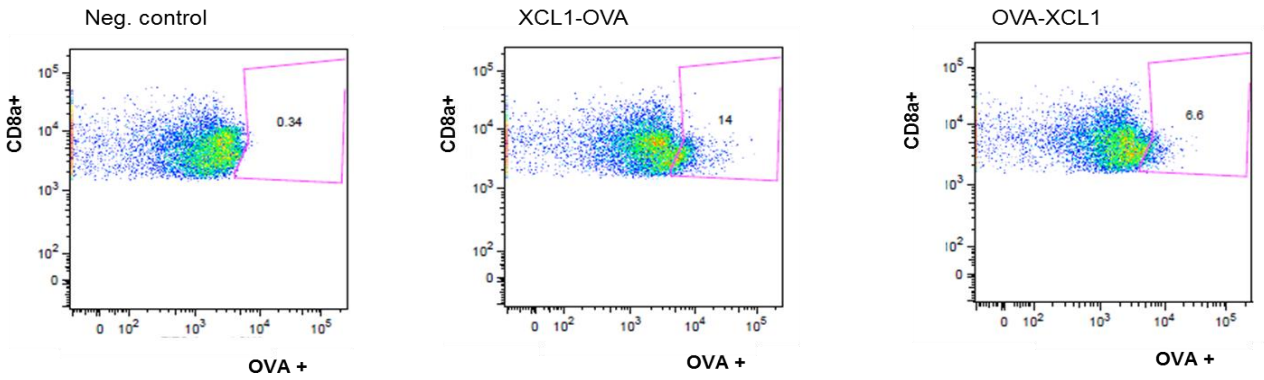

Figure 32

Binding of the different fusion constructs to DCs

Binding to DCs of the different OVA fusion proteins was detected by an OVA-specific, FITC-labeled secondary antibody. Each of the 3 fusion construct was compared to its variant in which OVA is at the N-terminus for its binding activity. The dot plots represent the percentage of cells CD8+ and OVA positive among the CD11c/MHCII + cells.

DISCUSSION

SAM vaccines are emerging as a novel class of nucleic acid-based vaccines. They offer the advantage of being fully synthetic and to combine the positive attributes of live-attenuated vaccines, while avoiding some of their limitations. Self-amplifying mRNA vaccines are considered a promising technology platform able to generate potent, versatile and easily produced vaccines to address the health challenges of the 21st century [66, 67, 70, 71, 79].

The mechanism by which SAM vaccines activate the host immune system has not been deeply investigated. Recently published data suggests that bone marrow derived Antigen Presenting Cells (APCs) are responsible for CD8 T cell priming after SAM vaccination. Since muscle fibers express antigens after SAM immunization, but APCs are not directly transfected by the SAM construct, cross-priming is proposed as the key mechanism for antigen presentation by SAM vaccines. Understanding the mechanism of action of these vaccines may enable to improve their efficacy.

The aim of the current study was to explore strategies to further potentiate the SAM platform. Assuming the pivotal role of APCs for the induction of the immune response, and taking into account the low amount of APCs present at the injection site, we investigated the possibility to enhance the immune response induced by SAM after the first immunization by increasing the recruitment of APCs at the site of injection.

In the last years this strategy has been deeply investigated and the enhancement in the number of APCs has been obtained in different ways and using different chemoattractants; in particular, GM-CSF has been selected among different possible molecules as an important hematopoietic growth factor and immune modulator and for its ability to induce maturation, migration, differentiation of Dendritic cells. GM-CSF has already been applied as immune adjuvant in many studies and in multiple vaccine platforms.

Our goal was to investigate whether an increase in the number of Antigen presenting cells at the injection site could improve the immunogenicity to a model antigen by using GM-CSF expressed by SAM vector as chemoattractant.

The model antigen selected for the study was Ovalbumin protein in a preliminary phase of the project, while in a second phase we moved to the Nucleoprotein from Influenza A Virus, in order to obtain a more complete set of data on the immunogenicity and to investigate also the effect of SAM(GM-CSF) on the protective efficacy after an Influenza challenge.

We have demonstrated that co-administration of SAM(GM-CSF) with SAM(OVA) is able to induce a significantly higher recruitment of immune cells compared to a combination of SAM(OVA)+ SAM(GFP). This recruitment was observed at the injection site, while in the lymph nodes small changes in cell numbers were detected. SAM(GFP) , an unrelated RNA, was added to SAM(OVA) for the control group, since it was known that the RNA formulated with CNE56 was able itself to induce a recruitment of immune cells. The majority of cells recruited at the injection site were antigen presenting cells, in particular Dendritic cells, Macrophages and Monocytes. The recruitment was continuously raising along the time-course, until day 3 after the immunization, leaving open the question on the duration of this immune cells recruitment. For this purpose, another *in vivo* recruitment study was performed to evaluate the infiltration of immune cells at the injection site along 24 days after the immunization. We have also decided to use a more appropriate negative control for the experiment; instead of the GFP, we co-administered with OVA a mutant form of GM-CSF that proved to be biologically inactive. The time course showed that the recruitment of APCs peaked at day 4 after the immunization and then started to decrease at day 7 returning to baseline levels at day 10. At the level of draining lymph node, only the population of monocytes showed a significant increase at day 3 in the group of mice immunized with SAM(GM-CSF).

We next wanted to evaluate whether the enhanced recruitment of APCs at the injection site could be related to an increase in the immunogenicity. We showed that mice immunized with SAM(GM-CSF) + SAM (OVA) induced a higher % of OVA-specific CD8+ T cells compared to mice immunized with SAM(OVA) + SAM(GFP), 10 days after the immunization. We did not observe any OVA-specific CD4+ T cell response specific to, probably due to the low dose of SAM(OVA)

administered. This effect correlated to the Antibody response: no detectable IgG titers 3 weeks after the immunization. In order to better characterize the immune response after SAM(GMCSF) administration, we decided to repeat the set of experiments with another antigen: we selected the Nucleoprotein antigen, since it proved in our hands to have high antigen-specific $CD8^+$ and $CD4^+$ T-cell response as well as high antibody titers after one immunization with low doses of RNA.

We confirmed the data previously obtained on the recruitment study with OVA as antigen also in mice immunized with SAM(NP) + SAM(GM-CSF) compared to mice immunized with SAM(NP) + SAM(mutGM-CSF). Indeed, the same trend of increase of the same populations was observed; thus, changing the antigen does not modify the effect of SAM (GM-CSF). The cellular immune response induced by SAM(GM-CSF) was assessed also for NP antigen. The co-administration of SAM(GM-CSF) with SAM(NP) was able to induce a significant increase in the number of $CD8^+$ T cells with a cytotoxic profile, compared to SAM(NP) + SAM(mutGM-CSF) co-administration or to SAM(NP) only administration. Moreover, we demonstrated that the cytotoxic CD8+ T cells induced by SAM(GM-CSF) have an enhanced cytotoxic activity *in vivo*.

At the level of NP-specific CD4+ T cells, only a slight increase was observed when mice were immunized with SAM(GM-CSF) + SAM(NP). This result was confirmed by the levels of NP-specific IgG titers. Indeed, SAM(GM-CSF) did not induce an increase in the Antibody titers. Moreover, on the basis of previous studies related to the timing of GM-CSF administration and its influence on the immune response, and considering the enhanced recruitment of APCs at day 3-4 after the immunization, we questioned whether the administration of SAM(GM-CSF) 3 days before the administration of the NP antigen, could further improve the presentation of the antigen and therefore potentiate the immune response. The data show that prior administration of SAM(GM-CSF) abolishes the increase on CD8+ T cells, thus suggesting that SAM(GM-CSF) better exerts its beneficial effect on the cellular response when it is co-administered with the antigen.

Finally, we studied the protective efficacy induced by SAM(GM-CSF) after the Influenza challenge, but this topic has to be further investigated, since in two parallel experiments performed, mice from the control group showed a high survival rate (75%) and a limited body weight loss at the peak of infection (10%), suggesting a very modest infection level. Nevertheless, in both experiments a

trend of better fitness was observed in mice immunized with SAM(NP) + SAM(GM-CSF) with respect to mice immunized with SAM(NP) or SAM(NP)+SAM(mutGM-CSF).

Overall, these findings suggest the adjuvant role of the SAM(GM-CSF) on the induction of the CD8+ T cell response; This suggest that the use of a chemo attractant that induces a recruitment of APCs at the injection site could help generating a stronger cellular response, probably acting on cross presentation. The increase in the number of Antigen presenting cells seems to have a beneficial effect especially on the cross presentation.

Overall, these findings suggest that the co-administration of a chemoattractant, in this case GM-CSF, able to induce a recruitment of APCs at the injection site, could help in generating a stronger cellular response upon SAM vaccination, probably mediated by an enhancement of the antigen cross-presentation.

In this study, we offered an alternative strategy to potentiate the SAM Vaccine Platform.

Although the Platform has already proven to be efficient in inducing both humoral and cellular immune responses, here we showed that increasing the number of APCs at the injection site was a successful approach to obtain an improvement in the cellular response: a single immunization of a low dose of SAM(GM-CSF) was able to elicit a more potent cytotoxic T cell response.

In this study, we selected GM-CSF as chemoattractant exclusively to reach the proof of concept. Indeed, caution must be taken when injecting a chemokine like GM-CSF as vaccine adjuvant. Various studies have been performed to evaluate potential mechanisms of GM-CSF-induced immunosuppression and there is still a debat regarding the use of GM-CSF as an immunoadjuvant [96].

The capacity of SAM vaccines to elicit a broad spectrum of protective immune response against both viral and bacterial pathogens, together with the synthetic methods to produce RNA and the potential to rapidly manufacture a large supply, make them a strong platform; moreover the possibility to further potentiate the cellular response by increasing the number of APCs at the injection site after a single immunization is of particular interest for preparedness for pandemics or outbreaks.

BIBLIOGRAPHY

[1] **Liu MA**. Immunologic basis of vaccine vectors. *Immunity*. 2010 Oct 29;33(4):504-15.

[2] **Geall AJ, Mandl CW, Ulmer JB**. RNA: the new revolution in nucleic acid vaccines. *Semin Immunol*. 2013 Apr; 25(2):152-9.

[3] **Ewer KJ, Lambe T, Rollier CS, Spencer AJ, Hill AV, Dorrell L**. Viral vectors as vaccine platforms: from immunogenicity to impact. *Curr Opin Immunol*. 2016 Aug; 41:47-54.

[4] **Wolff JA, Malone RW, Williams P, Chong W, Acsadi G, Jani A, Felgner PL**. Direct gene transfer into mouse muscle in vivo. *Science*. 1990 Mar 23; 247(4949 Pt 1):1465-8.

[5] **Chow YH, Chiang BL, Lee YL, Chi WK, Lin WC, Chen YT, Tao MH**. Development of Th1 and Th2 populations and the nature of immune responses to hepatitis B virus DNA vaccines can be modulated by codelivery of various cytokine genes. *J Immunol*.1998 Feb 1;160(3):1320-9.

[6] **Ulmer JB, Donnelly JJ, Parker SE, Rhodes GH, Felgner PL, Dwarki VJ, Gromkowski SH, Deck RR, DeWitt CM, Friedman A, et al**. Heterologous protection against influenza by injection of DNA encoding a viral protein. *Science*. 1993 Mar 19; 259 (5102):1745-9.

[7] **Klinman DM, Yamshchikov G, Ishigatsubo Y**. Contribution of CpG motifs to the immunogenicity of DNA vaccines. *J Immunol*. 1997 Apr 15;158(8):3635-9.

[8] **Ferraro B, Morrow MP, Hutnick NA, Shin TH, Lucke CE, Weiner DB**. Clinical applications of DNA vaccines: current progress. *Clin Infect Dis*. 2011 Aug 1; 53(3):296-302.

[9] **Kutzler MA, Weiner DB**. DNA vaccines: ready for prime time? *Nat Rev Genet*. 2008 Oct;9(10):776-88.

[10] **Pascolo S**. Messenger RNA-based vaccines. *Expert Opin Biol Ther*. 2004 Aug;4(8):1285-94.

[11] **Ulmer JB, Mason PW, Geall A, Mandl CW**. RNA-based vaccines. *Vaccine*. 2012 Jun 22; 30(30):4414-8.

[12] **Petsch B, Schnee M, Vogel AB, Lange E, Hoffmann B, Voss D, Schlake T, Thess A, Kallen KJ, Stitz L, Kramps T**. Protective efficacy of in vitro synthesized, specific mRNA vaccines against influenza A virus infection. *Nat Biotechnol*. 2012 Dec; 30(12):1210-6.

[13] **Mandl CW, Aberle JH, Aberle SW, Holzmann H, Allison SL, Heinz FX**. In vitro-synthesized infectious RNA as an attenuated live vaccine in a flavivirus model. *Nat Med*. 1998 Dec; 4(12):1438-40.

[14] **Jin B, Sun T, Yu XH, Liu CQ, Yang YX, Lu P, Fu SF, Qiu HB, Yeo AE**. Immunomodulatory effects of dsRNA and its potential as vaccine adjuvant. *J Biomed Biotechnol*. 2010; 2010:690438.

[15] **Caskey M, Lefebvre F, Filali-Mouhim A, Cameron MJ, Goulet JP, Haddad EK, Breton G, Trumpfheller C, Pollak S, Shimeliovich I, Duque-Alarcon A, Pan L, Nelkenbaum A, Salazar AM, Schlesinger SJ, Steinman RM, Sékaly RP**. Synthetic double-stranded RNA induces innate immune responses similar to a live viral vaccine in humans. *J Exp Med*. 2011 Nov 21; 208(12):2357-66.

[16] **Wang Y, Swiecki M, McCartney SA, Colonna M**. dsRNA sensors and plasmacytoid dendritic cells in host defense and autoimmunity. *Immunol Rev*. 2011 Sep; 243(1):74-90.

[17] **Johansson DX, Ljungberg K, Kakoulidou M, Liljeström P**. Intradermal electroporation of naked replicon RNA elicits strong immune responses. *PLoS One*. 2012; 7(1):e29732.

[18] **Atkins GJ, Fleeton MN, Sheahan BJ**. Therapeutic and prophylactic applications of alphavirus vectors. *Expert Rev Mol Med*. 2008 Nov 11; 10:e33.

[19] **Lundstrom K**. Alphavirus vectors: applications for DNA vaccine production and gene expression. *Intervirology*. 2000; 43(4-6):247-57.

[20] **Schlesinger S**. Alphavirus vectors: development and potential therapeutic applications. *Expert Opin Biol Ther.* 2001 Mar; 1(2):177-91.

[21] **Tannis LL, Gauthier A, Evelegh C, Parsons R, Nyholt D, Khromykh A, Bramson JL**. Semliki forest virus and Kunjin virus RNA replicons elicit comparable cellular immunity but distinct humoral immunity. *Vaccine*. 2005 Jul 21; 23(33):4189-94.

[22] **Mossman SP, Bex F, Berglund P, Arthos J, O'Neil SP, Riley D, Maul DH, Bruck C, Momin P, Burny A, Fultz PN, Mullins JI, Liljeström P, Hoover EA**. Protection against lethal simian immunodeficiency virus SIVsmmPBj14 disease by a recombinant Semliki Forest virus gp160 vaccine and by a gp120 subunit vaccine. *J Virol*. 1996 Mar;70(3):1953-60.

[23] **Carroll TD, Matzinger SR, Barro M, Fritts L, McChesney MB, Miller CJ, Johnston RE**. Alphavirus replicon-based adjuvants enhance the immunogenicity and effectiveness of Fluzone ® in rhesus macaques. *Vaccine.* 2011 Jan 29; 29(5):931-40.

[24] **Bernstein DI, Reap EA, Katen K, Watson A, Smith K, Norberg P, Olmsted RA, Hoeper A, Morris J, Negri S, Maughan MF, Chulay JD**. Randomized, double-blind, Phase 1 trial of an alphavirus replicon vaccine for cytomegalovirus in CMV seronegative adult volunteers. *Vaccine*. 2009 Dec 11; 28(2):484-93.

[25] **Brito LA, Chan M, Shaw CA, Hekele A, Carsillo T, Schaefer M, Archer J, Seubert A, Otten GR, Beard CW, Dey AK, Lilja A, Valiante NM, Mason PW, Mandl CW, Barnett SW, Dormitzer PR, Ulmer JB, Singh M, O'Hagan DT, Geall AJ**. A cationic nanoemulsion for the delivery of next-generation RNA vaccines. *Mol Ther*. 2014 Dec; 22(12):2118-29.

[26] **Deering RP, Kommareddy S, Ulmer JB, Brito LA, Geall AJ**. Nucleic acid vaccines: prospects for non-viral delivery of mRNA vaccines. *Expert Opin Drug Deliv*. 2014 Jun; 11(6):885-99.

[27] **Perri S, Greer CE, Thudium K, Doe B, Legg H, Liu H, Romero RE, Tang Z, Bin Q, Dubensky TW Jr, Vajdy M, Otten GR, Polo JM**. An alphavirus replicon particle chimera derived from venezuelan equine encephalitis and sindbis viruses is a potent gene-based vaccine delivery vector. *J Virol*. 2003 Oct; 77(19):10394-403.

[28] **Kofler RM, Aberle JH, Aberle SW, Allison SL, Heinz FX, Mandl CW**. Mimicking live flavivirus immunization with a noninfectious RNA vaccine. *Proc Natl Acad Sci* U S A. 2004 Feb 17; 101(7):1951-6.

[29] **Smerdou C, Liljeström P**. Non-viral amplification systems for gene transfer: vectors based on alphaviruses. *Curr Opin Mol Ther*. 1999 Apr; 1(2):244-51.

[30] **Rayner JO, Dryga SA, Kamrud KI**. Alphavirus vectors and vaccination. *Rev Med Virol*. 2002 Sep-Oct; 12(5):279-96.

[31] **Semple SC, Akinc A, Chen J, Sandhu AP, Mui BL, Cho CK, Sah DW, Stebbing D, Crosley EJ, Yaworski E, Hafez IM, Dorkin JR, Qin J, Lam K, Rajeev KG, Wong KF, Jeffs LB, Nechev L, Eisenhardt ML, Jayaraman M, Kazem M, Maier MA, Srinivasulu M, Weinstein MJ, Chen Q, Alvarez R, Barros SA, De S, Klimuk SK, Borland T, Kosovrasti V, Cantley WL, Tam YK, Manoharan M, Ciufolini MA, Tracy MA, de Fougerolles A, MacLachlan I, Cullis PR, Madden TD, Hope MJ**. Rational design of cationic lipids for siRNA delivery. *Nat Biotechnol*. 2010 Feb; 28(2):172-6.

[32] **Whitehead KA, Langer R, Anderson DG**. Knocking down barriers: advances in siRNA delivery. *Nat Rev Drug Discov*. 2009 Feb;8(2):129-38.

[33] **Geall AJ, Verma A, Otten GR, Shaw CA, Hekele A, Banerjee K, Cu Y, Beard CW, Brito LA, Krucker T, O'Hagan DT, Singh M, Mason PW, Valiante NM, Dormitzer PR, Barnett SW, Rappuoli R, Ulmer JB, Mandl CW**. Nonviral

delivery of self-amplifying RNA vaccines. *Proc Natl Acad Sci* U S A. 2012 Sep 4; 109(36):14604-9.

[34] **Bogers WM, Oostermeijer H, Mooij P, Koopman G, Verschoor EJ, Davis D, Ulmer JB, Brito LA, Cu Y, Banerjee K, Otten GR, Burke B, Dey A, Heeney JL, Shen X, Tomaras GD, Labranche C, Montefiori DC, Liao HX, Haynes B, Geall AJ, Barnett SW**. Potent immune responses in rhesus macaques induced by nonviral delivery of a self-amplifying RNA vaccine expressing HIV type 1 envelope with a cationic nanoemulsion. J *Infect Dis*. 2015 Mar 15; 211(6):947-55.

[35] **Hekele A, Bertholet S, Archer J, Gibson DG, Palladino G, Brito LA, Otten GR, Brazzoli M, Buccato S, Bonci A, Casini D, Maione D, Qi ZQ, Gill JE, Caiazza NC, Urano J, Hubby B, Gao GF, Shu Y, De Gregorio E, Mandl CW, Mason PW, Settembre EC, Ulmer JB, Craig Venter J, Dormitzer PR, Rappuoli R, Geall AJ**. Rapidly produced SAM(®) vaccine against H7N9 influenza is immunogenic in mice. *Emerg Microbes Infect*. 2013 Aug; 2(8):e52.

[36] **Lazzaro S, Giovani C, Mangiavacchi S, Magini D, Maione D, Baudner B, Geall AJ, De Gregorio E, D'Oro U, Buonsanti C**. CD8 T-cell priming upon mRNA vaccination is restricted to bone-marrow-derived antigen-presenting cells and may involve antigen transfer from myocytes. *Immunology*. 2015 Oct; 146(2):312-26.

[37] **Bevan MJ**. Cross-priming for a secondary cytotoxic response to minor H antigens with H-2 congenic cells which do not cross-react in the cytotoxic assay. *J Exp Med*. 1976 May 1; 143(5):1283-8.

[38] **Huang AY, Golumbek P, Ahmadzadeh M, Jaffee E, Pardoll D, Levitsky H**. Role of bone marrow-derived cells in presenting MHC class I-restricted tumor antigens. *Science*. 1994 May 13; 264(5161):961-5.

[39] **Sigal LJ, Crotty S, Andino R, Rock KL**. Cytotoxic T-cell immunity to virus-infected non-haematopoietic cells requires presentation of exogenous antigen. *Nature*. 1999 Mar 4; 398(6722):77-80.

[40] **Yewdell JW, Haeryfar SM**. Understanding presentation of viral antigens to CD8+ T cells in vivo: the key to rational vaccine design. *Annu Rev Immunol*. 2005; 23:651-82..

[41] **Albert ML, Sauter B, Bhardwaj N**. Dendritic cells acquire antigen from apoptotic cells and induce class I-restricted CTLs. *Nature*. 1998 Mar 5; 392(6671):86-9.

[42] **Bellone M, Iezzi G, Rovere P, Galati G, Ronchetti A, Protti MP, Davoust J, Rugarli C, Manfredi AA**. Processing of engulfed apoptotic bodies yields T cell epitopes. *J Immunol*. 1997 Dec 1; 159(11):5391-9.

[43] **Arrode G, Boccaccio C, Lulé J, Allart S, Moinard N, Abastado JP, Alam A, Davrinche C**. Incoming human cytomegalovirus pp65 (UL83) contained in apoptotic infected fibroblasts is cross-presented to CD8(+) T cells by dendritic cells. *J Virol*. 2000 Nov; 74(21):10018-24.

[44] **Lu Z, Yuan L, Zhou X, Sotomayor E, Levitsky HI, Pardoll DM**. CD40-independent pathways of T cell help for priming of CD8(+) cytotoxic T lymphocytes. *J Exp Med*. 2000 Feb 7; 191(3):541-50.

[45] **den Haan JM, Lehar SM, Bevan MJ**. CD8(+) but not CD8(-) dendritic cells cross-prime cytotoxic T cells in vivo. *J Exp Med*. 2000 Dec 18; 192(12):1685-96.

[46] **Burgdorf S, Kautz A, Böhnert V, Knolle PA, Kurts C**. Distinct pathways of antigen uptake and intracellular routing in CD4 and CD8 T cell activation. *Science*. 2007 Apr 27; 316(5824):612-6.

[47] **Dudziak D, Kamphorst AO, Heidkamp GF, Buchholz VR, Trumpfheller C, Yamazaki S, Cheong C, Liu K, Lee HW, Park CG, Steinman RM, Nussenzweig MC**. Differential antigen processing by dendritic cell subsets in vivo. *Science*. 2007 Jan 5; 315(5808):107-11.

[48] **Burgdorf S, Kurts C**. Endocytosis mechanisms and the cell biology of antigen presentation. *Curr Opin Immunol*. 2008 Feb; 20(1):89-95.

[49] **Caminschi I, Proietto AI, Ahmet F, Kitsoulis S, Shin Teh J, Lo JC, Rizzitelli A, Wu L, Vremec D, van Dommelen SL, Campbell IK, Maraskovsky E, Braley H, Davey GM, Mottram P, van de Velde N, Jensen K, Lew AM, Wright MD, Heath WR, Shortman K, Lahoud MH**. The dendritic cell subtype-restricted C-type lectin Clec9A is a target for vaccine enhancement. *Blood*. 2008 Oct 15; 112(8):3264-73.

[50] **Weck MM, Appel S, Werth D, Sinzger C, Bringmann A, Grünebach F, Brossart P**. hDectin-1 is involved in uptake and cross-presentation of cellular antigens. *Blood*. 2008 Apr 15;111(8):4264-72.

[51] **Kroczek RA, Henn V**. The Role of XCR1 and its Ligand XCL1 in Antigen Cross-Presentation by Murine and Human Dendritic Cells. *Front Immunol*. 2012 Feb 10; 3:14.

[52] **Bodey GP**. The potential role of granulocyte-macrophage colony stimulating factor in therapy of fungal infections: a commentary. *Eur J Clin Microbiol Infect Dis*. 1994 May; 13(5):363-6.

[53] **Jäger E, Ringhoffer M, Dienes HP, Arand M, Karbach J, Jäger D, Ilsemann C, Hagedorn M, Oesch F, Knuth A**. Granulocyte-macrophage-colony-stimulating factor enhances immune responses to melanoma-associated peptides in vivo. *Int J Cancer*. 1996 Jul 3; 67(1):54-62.

[54] **Disis ML, Bernhard H, Shiota FM, Hand SL, Gralow JR, Huseby ES, Gillis S, Cheever MA**. Granulocyte-macrophage colony-stimulating factor: an effective adjuvant for protein and peptide-based vaccines. *Blood*. 1996 Jul 1; 88(1):202-10.

[55] **Steinman RM**. The dendritic cell system and its role in immunogenicity. *Annu Rev Immunol*. 1991; 9:271-96.

[56] **Dranoff G, Jaffee E, Lazenby A, Golumbek P, Levitsky H, Brose K, Jackson V, Hamada H, Pardoll D, Mulligan RC**. Vaccination with irradiated tumor cells engineered to secrete murine granulocyte-macrophage colony-stimulating factor stimulates potent, specific, and long-lasting anti-tumor immunity. *Proc Natl Acad Sci* U S A. 1993 Apr 15; 90(8):3539-43.

[57] **Tarr PE, Lin R, Mueller EA, Kovarik JM, Guillaume M, Jones TC**. Evaluation of tolerability and antibody response after recombinant human granulocyte-macrophage colony-stimulating factor (rhGM-CSF) and a single dose of recombinant hepatitis B vaccine. *Vaccine.* 1996 Sep; 14(13):1199-204.

[58] **Kurzrock R, Talpaz M, Gutterman JU**. Very low doses of GM-CSF administered alone or with erythropoietin in aplastic anemia. *Am J Med*. 1992 Jul; 93(1):41-8.

[59] **Estey EH, Kurzrock R, Talpaz M, McCredie KB, O'Brien S, Kantarjian HM, Keating MJ, Deisseroth AB, Gutterman JU**. Effects of low doses of recombinant human granulocyte-macrophage colony stimulating factor (GM-CSF) in patients with myelodysplastic syndromes. *Br J Haematol*. 1991 Mar; 77(3):291-5.

[60] **McNeel DG, Schiffman K, Disis ML**. Immunization with recombinant human granulocyte-macrophage colony-stimulating factor as a vaccine adjuvant elicits both a cellular and humoral response to recombinant human granulocyte-macrophage colony-stimulating factor. *Blood*. 1999 Apr 15; 93(8):2653-9.

[61] **Disis ML, Bernhard H, Shiota FM, Hand SL, Gralow JR, Huseby ES, Gillis S, Cheever MA**. Granulocyte-macrophage colony-stimulating factor: an effective adjuvant for protein and peptide-based vaccines. *Blood*. 1996 Jul 1; 88(1):202-10.

[62] **Liu Y, Xiao L, Joo KI, Hu B, Fang J, Wang P**. In situ modulation of dendritic cells by injectable thermosensitive hydrogels for cancer vaccines in mice. *Biomacromolecules*. 2014 Oct 13; 15(10):3836-45.

[63] **Noh KH, Park YM, Kim HS, Kang TH, Song KH, Lee YH, Byeon Y, Jeon HN, Jung ID, Shin BC, Lee KM, Seong SY, Han HD, Kim TW**. GM-CSF-loaded chitosan hydrogel as an immunoadjuvant enhances antigen-specific immune responses with reduced toxicity. *BMC Immunol*. 2014 Oct 18; 15:48.

[64] **Labeur MS, Roters B, Pers B, Mehling A, Luger TA, Schwarz T, Grabbe S**. Generation of tumor immunity by bone marrow-derived dendritic cells correlates with dendritic cell maturation stage. *J Immunol*. 1999 Jan 1; 162(1):168-75.

[65] **Nestle FO, Alijagic S, Gilliet M, Sun Y, Grabbe S, Dummer R, Burg G, Schadendorf D**. Vaccination of melanoma patients with peptide- or tumor lysate-pulsed dendritic cells. *Nat Med*. 1998 Mar; 4(3):328-32.

[66] **Curiel-Lewandrowski C, Mahnke K, Labeur M, Roters B, Schmidt W, Granstein RD, Luger TA, Schwarz T, Grabbe S**. Transfection of immature murine bonemarrow-derived dendritic cells with the granulocyte-macrophage colony-stimulating factor gene potently enhances their in vivo antigen-presenting capacity. *J Immunol*. 1999 Jul 1; 163(1):174-83.

[67] **Gerloni M, Lo D, Ballou WR, Zanetti M**. Immunological memory after somatic transgene immunization is positively affected by priming with GM-CSF and does not require bone marrow-derived dendritic cells. *Eur J Immunol*. 1998 Jun; 28(6):1832-8.

[68] **Lee SW, Cho JH, Sung YC**. Optimal induction of hepatitis C virus envelope-specific immunity by bicistronic plasmid DNA inoculation with the granulocyte-macrophage colony-stimulating factor gene. *J Virol*. 1998 Oct; 72(10):8430-6.

[69] **Xiang Z, Ertl HC**. Manipulation of the immune response to a plasmid-encoded viral antigen by coinoculation with plasmids expressing cytokines. *Immunity*. 1995 Feb; 2(2):129-35.

[70] **Kim JJ, Ayyavoo V, Bagarazzi ML, Chattergoon MA, Dang K, Wang B, Boyer JD, Weiner DB**. In vivo engineering of a cellular immune response by coadministration of IL-12 expression vector with a DNA immunogen. *J Immunol*. 1997 Jan 15; 158(2):816-26.

[71] **Iwasaki A, Stiernholm BJ, Chan AK, Berinstein NL, Barber BH**. Enhanced CTL responses mediated by plasmid DNA immunogens encoding costimulatory molecules and cytokines. *J Immunol*. 1997 May 15; 158(10):4591-601.

[72] **Geissler M, Gesien A, Tokushige K, Wands JR**. Enhancement of cellular and humoral immune responses to hepatitis C virus core protein using DNA-based vaccines augmented with cytokine-expressing plasmids. *J Immunol*. 1997 Feb 1; 158(3):1231-7.

[73] **Cho JH, Lee SW, Sung YC**. Enhanced cellular immunity to hepatitis C virus nonstructural proteins by codelivery of granulocyte macrophage-colony stimulating factor gene in intramuscular DNA immunization. *Vaccine*. 1999 Mar 5; 17(9-10):1136-44.

[74] **Weiss WR, Ishii KJ, Hedstrom RC, Sedegah M, Ichino M, Barnhart K, Klinman DM, Hoffman SL**. A plasmid encoding murine granulocyte-macrophage colony-stimulating factor increases protection conferred by a malaria DNA vaccine. *J Immunol*. 1998 Sep 1; 161(5):2325-32.

[75] **Tacken PJ, de Vries IJ, Torensma R, Figdor CG**. Dendritic-cell immunotherapy: from ex vivo loading to in vivo targeting. *Nat Rev Immunol*. 2007 Oct; 7(10):790-802.

[76] **Steinman RM, Banchereau J**. Taking dendritic cells into medicine. Nature. 2007 Sep 27; 449(7161):419-26.

[77] **Kastenmüller W, Kastenmüller K, Kurts C, Seder RA**. Dendritic cell-targeted vaccines--hope or hype? *Nat Rev Immunol*. 2014 Oct; 14(10):705-11.

[78] **Snider DP, Segal DM**. Targeted antigen presentation using crosslinked antibody heteroaggregates. *J Immunol*. 1987 Sep 1; 139(5):1609-16.

[79] **Carayanniotis G, Barber BH**. Adjuvant-free IgG responses induced with antigen coupled to antibodies against class II MHC. *Nature*. 1987 May 7-13; 327(6117):59-61.

[80] **Frleta D, Demian D, Wade WF**. Class II-targeted antigen is superior to CD40-targeted antigen at stimulating humoral responses in vivo. *Int Immunopharmacol*. 2001 Feb; 1(2):265-75.

[81] **Dudziak D, Kamphorst AO, Heidkamp GF, Buchholz VR, Trumpfheller C, Yamazaki S, Cheong C, Liu K, Lee HW, Park CG, Steinman RM, Nussenzweig MC**. Differential antigen processing by dendritic cell subsets in vivo. *Science.* 2007 Jan 5;315(5808):107-11.

[82] **Bachem A, Güttler S, Hartung E, Ebstein F, Schaefer M, Tannert A, Salama A, Movassaghi K, Opitz C, Mages HW, Henn V, Kloetzel PM, Gurka S, Kroczek RA**. Superior antigen cross-presentation and XCR1 expression define human CD11c+CD141+ cells as homologues of mouse CD8+ dendritic cells. *J Exp Med*. 2010 Jun 7; 207(6):1273-81.

[83] **Crozat K, Guiton R, Contreras V, Feuillet V, Dutertre CA, Ventre E, Vu Manh TP, Baranek T, Storset AK, Marvel J, Boudinot P, Hosmalin A, Schwartz-Cornil I, Dalod M**. The XC chemokine receptor 1 is a conserved selective marker of mammalian cells homologous to mouse CD8alpha+ dendritic cells. *J Exp Med*. 2010 Jun 7; 207(6):1283-92.

[84] **Jongbloed SL, Kassianos AJ, McDonald KJ, Clark GJ, Ju X, Angel CE, Chen CJ, Dunbar PR, Wadley RB, Jeet V, Vulink AJ, Hart DN, Radford KJ**. Human CD141+ (BDCA-3)+ dendritic cells (DCs) represent a unique myeloid DC

subset that cross-presents necrotic cell antigens. *J Exp Med*. 2010 Jun 7; 207(6):1247-60.

[85] **Poulin LF, Salio M, Griessinger E, Anjos-Afonso F, Craciun L, Chen JL, Keller AM, Joffre O, Zelenay S, Nye E, Le Moine A, Faure F, Donckier V, Sancho D, Cerundolo V, Bonnet D, Reis e Sousa C**. Characterization of human DNGR-1+ BDCA3+ leukocytes as putative equivalents of mouse CD8alpha+ dendritic cells. *J Exp Med*. 2010 Jun 7; 207(6):1261-71.

[86] **Sancho D, Mourão-Sá D, Joffre OP, Schulz O, Rogers NC, Pennington DJ, Carlyle JR, Reis e Sousa C**. Tumor therapy in mice via antigen targeting to a novel, DC-restricted C-type lectin. *J Clin Invest*. 2008 Jun; 118(6):2098-110.

[87] **Chatterjee B, Smed-Sörensen A, Cohn L, Chalouni C, Vandlen R, Lee BC, Widger J, Keler T, Delamarre L, Mellman I**. Internalization and endosomal degradation of receptor-bound antigens regulate the efficiency of cross presentation by human dendritic cells. *Blood*. 2012 Sep 6; 120(10):2011-20.

[88] **Cohn L, Chatterjee B, Esselborn F, Smed-Sörensen A, Nakamura N, Chalouni C, Lee BC, Vandlen R, Keler T, Lauer P, Brockstedt D, Mellman I, Delamarre L**. Antigen delivery to early endosomes eliminates the superiority of human blood BDCA3+ dendritic cells at cross presentation. *J Exp Med*. 2013 May 6; 210(5):1049-63.

[89] **Burgdorf S, Kautz A, Böhnert V, Knolle PA, Kurts C**. Distinct pathways of antigen uptake and intracellular routing in CD4 and CD8 T cell activation. *Science*. 2007 Apr 27; 316(5824):612-6.

[90] **Meropol NJ, Altmann SW, Shanafelt AB, Kastelein RA, Johnson GD, Prystowsky MB**. Requirement of hydrophilic amino-terminal residues for granulocyte-macrophage colony-stimulating factor bioactivity and receptor binding. *J Biol Chem*. 1992 Jul 15; 267(20):14266-9.

[91] **Magini D, Giovani C, Mangiavacchi S, Maccari S, Cecchi R, Ulmer JB, De Gregorio E, Geall AJ, Brazzoli M, Bertholet S**. Self-Amplifying mRNA Vaccines Expressing Multiple Conserved Influenza Antigens Confer Protection against Homologous and Heterosubtypic Viral Challenge. *PLoS One*. 2016 Aug 15; 11(8):e0161193.

[92] **Rush C, Mitchell T, Garside P**. Efficient priming of CD4+ and CD8+ T cells by DNA vaccination depends on appropriate targeting of sufficient levels of immunologically relevant antigen to appropriate processing pathways. *J Immunol*. 2002 Nov 1; 169(9):4951-60.

[93] **Inaba K, Inaba M, Romani N, Aya H, Deguchi M, Ikehara S, Muramatsu S, Steinman RM**. Generation of large numbers of dendritic cells from mouse bone

marrow cultures supplemented with granulocyte/macrophage colony-stimulating factor. *J Exp Med*. 1992 Dec 1; 176(6):1693-702.

[94] **Stambas J, Doherty PC, Turner SJ**. An in vivo cytotoxicity threshold for influenza A virus-specific effector and memory CD8(+) T cells. *J Immunol*. 2007 Feb 1; 178(3):1285-92.

[95] **Arras M, Glauser DL, Jirkof P, Rettich A, Schade B, Cinelli P, Pinschewer DD,**

Ackermann M. Multiparameter telemetry as a sensitive screening method to detect

vaccine reactogenicity in mice. *PLoS One*. 2012; 7(1):e29726.

[96] **Clive KS, Tyler JA, Clifton GT, Holmes JP, Mittendorf EA, Ponniah S, Peoples**

GE. Use of GM-CSF as an adjuvant with cancer vaccines: beneficial or detrimental?

Expert Rev Vaccines. 2010 May; 9(5):519-25.

Disclaimer

This work was sponsored and funded by GlaxoSmithKline Biologicals SA.
Cristina Manara is a PhD student at the University of Rome La Sapienza and participated in a Doctoral Program at GSK.